Out-of-plane behaviour of unreinforced masonry infill walls: Review of the experimental studies and analysis of the influencing parameters

Bharat Pradhan[a], Maria Zizzo[a], Vasilis Sarhosis[b], Liborio Cavaleri[a*]

[a]*Department of Engineering, University of Palermo, 90128 Palermo, Italy*

[b]*School of Civil Engineering, University of Leeds, LS2 9JT, Leeds, United Kingdom*

Abstract

Over the last 50 years, research has mainly focused on characterizing the In-Plane behaviour of unreinforced masonry infill walls. Recently, the focus of research has been addressed to understanding Out-of-Plane behaviour, also from the experimental point of view. However, in the experimental campaigns, there is high variability in the geometrical and mechanical properties of URM infill walls and also in the application of Out-of-Plane loads. Therefore, it is important to outline and critically evaluate the major findings obtained by experimental studies and identify research gaps to better understand the differences and the affinity of apparently equivalent tests. In this paper, the extensive literature regarding the Out-of-Plane tests on infill walls has been reviewed with a detailed comparison of the experimental results based on different influencing parameters (slenderness ratio, aspect ratio, boundary conditions, openings, vertical load, In-Plane damage, strength of masonry and plaster, frame stiffness). Based on the study, the main areas that demand further experimental campaigns have been identified and recommended.

Keywords

Experimental campaigns, Unreinforced Masonry Infill, Out-of-plane, In-Plane/Out-of-Plane Interaction, Out-of-Plane Strength, Review

[*] Corresponding author
E-mail address: liborio.cavaleri@unipa.it

1. Introduction

Studies have shown that unreinforced masonry (URM) infill walls (*hereafter also referred to as infills*) play a significant role in the seismic safety of modern buildings with reinforced concrete (RC) or steel frames. In the past, research established how masonry infills influence the In-Plane (IP) strength and stiffness of infilled frames and their collapse mechanism during an earthquake (e.g. Mehrabi et al. 1996, Cavaleri et al. 2005). Typical IP failures of infill walls have been understood and seismic safety of infilled frame structures considering them has been recommended in design codes worldwide. Research shows that during an earthquake, an interaction between the IP and Out-of-Plane (OOP) forces exists and IP and OOP damage occur simultaneously (e.g. Cavaleri et al 2019, Gesualdi et al 2020, Ricci et al 2020, Pradhan et al 2021). The post-earthquake damage surveys show that the OOP collapse of infill walls is critical even for new buildings designed to resist earthquakes, resulting in casualties and economic losses (Ricci et al. 2011; Hermanns et al. 2014; Barbosa et al. 2017; Varum et al. 2017). However, studies related to the OOP behaviour of infill walls are limited and there are still very few provisions to prevent OOP failure of infill walls in design codes like Eurocode 8 (2004) and ASCE 41 (2017). For example, Eurocode 8 (2004) recommends limiting the slenderness ratio of infills to 15. In cases where the ratio is higher, application of light wire meshes well anchored on one face of the wall, wall ties fixed to columns, concrete posts and belts across the panels are suggested to prevent OOP collapse. Experimental investigation by Wu et al. (2020) showed increased OOP seismic performance with the provisions of cast-in-place belt in the infill walls.

Past experimental studies have shown that the OOP capacity of infill walls is affected by arching action caused by confinement provided by the surrounding frame (Dawe and Seah 1989; Angel 1994; Flanagan and Bennett 1999b). Analytical models based on the arching mechanism, were thus proposed, to determine the OOP capacity of infill walls (McDowell et al. 1956; Dawe and Seah 1989; Angel 1994; Bashandy et al. 1995; Flanagan and Bennett 1999a). However, the OOP strength is highly influenced by the interacting nature of IP and OOP loads during an earthquake. An IP load can damage the mortar joint between frame and infill and can alter the boundary conditions (Furtado et al. 2016; Butenweg et al. 2019) and the failure patterns (Anić et al. 2019; Butenweg et al., 2019). Experimentally, it has been found that IP damage of infill walls can significantly reduce their OOP capacity (Angel 1994; Calvi and Bolognini 2001; Furtado et al. 2016; Ricci et al. 2018a). However, the decay of OOP strength due to IP damage is not straightforward. The rate of decay is also influenced by the slenderness ratio as well as masonry's strength (Agnihotri et al. 2013; Wang et al., 2020).

The extent of arching depends on the slenderness ratio of the infill walls. The lower the slenderness ratio, the higher the OOP strength of the infills (Dawe and Seah 1989; Angel 1994; Flanagan and Bennett 1999b; Ricci et al. 2018b). For highly slender infill walls, the arching mechanism is limited by a snap-through failure (Angel 1994; Moghadam and Goudarzi 2010). Arching is also influenced by the aspect ratio (length-to-height ratio) of infill walls. In fact, higher aspect ratio decreases the OOP capacity (Lunn and Rizkala 2011; Moreno-Herera et al. 2016). Vertical arching is also influenced by the level of the vertical pre-compression applied to the infill wall (Varela-Rivera et al. (2012b).

The OOP behaviour of infill walls is influenced by openings like doors and windows and such openings are unavoidable in buildings due to functional requirements. Experimental campaigns have shown that the OOP capacity can reduce due to openings (Dawe and Seah 1989; Akhoundi et al. 2016). ASCE 41 (2017) also recommends to take into account the reduction of the OOP capacity due to the openings.

Further, the OOP capacity of infills is affected by the stiffness of the surrounding frames (Angel 1994), and also by the strength of the masonry (Angel 1994; Moreno-Herera et al., 2016). In summary, the OOP behaviour of infill walls is complex as it depends upon several parameters associated with both the masonry infill and the surrounding frames. Given these complexities, past experimental studies have focused on how different parameters influence the OOP capacity of infill walls and it is necessary to compare the experimental findings in detail.

Research on correlating OOP experimental results has also progressed in recent years (e.g. Pasca et al. 2017; Furtado et al. 2018; Anić et al. 2019; Liberatore et al. 2020) whereby the reliability of the analytical models in describing the OOP capacity has also been compared. For example, Pasca et al. (2017) found the model by Flanagan and Bennett (1999a) better for the infill specimens tested by Dawe and Seah (1989) while it was found conservative for the confined masonry specimens tested by Varella-Rivera et al. (2012a). Similarly, Anić et al. (2019) observed that the models by Ricci et al. (2018c) and Moghadam and Goudarzi (2010) are relatively better for the case of infilled frames. While, Liberatore et al. (2020) found the equation in Eurocode 6 (2005), in average, better for the estimation of OOP capacity of masonry walls without frames, confined masonry walls or infill walls in RC frames.

A high effort has been made to assess the OOP strength as well as the stiffness basing on experimental results (Ricci et al. 2018c; Furtado et al. 2018; Liberatore et al. 2020). Nevertheless, the check of the accuracy of the existing analytical models or the development of any such model are affected by the number of tests and the types of masonry specimens considered (i.e. with or without frames). For this, the knowledge of the suitable experimental data, which can be achieved only through comparative assessment of experimental results, is always important.

Therefore, this paper is focused on the critical evaluation of the experimental efforts that have been carried out so far to understand the OOP behaviour of URM infill walls. For this, an extensive database of OOP experimental tests (more than 50) has been taken, and research gaps have been highlighted in terms of ranges of geometrical and mechanical properties of masonry not yet experimented in detail. Experimental results have been compared focusing on parameters influencing the OOP capacity (slenderness ratio, IP damage, aspect ratio, boundary conditions, openings, vertical load, strength of masonry, surface plaster, frame stiffness). With detailed analyses, the key parameters, to focus in the future experimental campaigns, have been identified and recommended.

It has to be underlined that no comparisons of the experimental results with the models proposed in the literature for the OOP capacity of infills will be here proposed because included in a further study.

2. Overview of the experimental campaigns in the literature

To understand the OOP behaviour of infill walls, available OOP experimental tests conducted on URM infill specimens in RC or steel frames have been analysed. OOP tests on masonry panels without frames available in the literature (e.g. Cavaleri et al. 2009) have not been considered here because these tests do not replicate in general the boundary conditions between frame and infill. Therefore, these are not useful for the scope of this paper. URM infilled frames under OOP loads in combination with IP loads have been also considered. Additionally, to augment the understandings, experimental campaigns on confined masonry (CM) walls surrounded with frames and tested under similar loading conditions, have been used (e.g. Varela-Rivera et al. 2011, Komaraneni et al. 2011, Moreno-Herera et al. 2016). The OOP behaviour of CM walls is similar to that of infill walls. In fact, OOP capacity of CM walls can be high due to the interaction between masonry and RC elements (Pasca et al. 2017). The difference between the two systems is that, in the infilled frame constructions, the infill walls are constructed after the frames, while in the other, the RC elements are constructed after the masonry walls.

For sake of completeness, among the listed experimental tests (Tab. 1), also those referred to infill specimens with some sort of strengthening like bed joint reinforcements, surface reinforcements, textile reinforced mortar, etc. (Dawe and Seah 1989; Pereira et al. 2011; Da Porto et al. 2013, Panto et al. 2019) are included. However, the experimental results obtained from such specimens have not been used for comparisons in this study, as the focus is on URM infills.

In the literature it is possible to find tests on new infill systems designed to reduce the vulnerability seen in the existing masonry infills. The construction techniques in these new infill types are different from infills used in practice. For example, Petrus et al. (2015) and Moşoarcă et al. (2016) tested masonry made with a consolidation technique. Preti et al. (2015) and Milanesi et al. (2020) have tested infill systems made with sliding joints, and others (Silva et al. 2016; Verlato et al. 2016; Vailati et al. 2018; Palieraki et al. 2018) proposed infill walls with masonry enclosure systems with a possibility of including horizontal or vertical steel reinforcements. Such new infill systems were found to be very efficient in both IP and OOP loads.

Table 1 lists some of the important details from the experimental studies considered in this study. It contains information about the types of frames, type of construction (infill or confined masonry), type of masonry units, direction of hole in hollow units, loading types, aspect ratios, slenderness ratios, boundary conditions (gaps with beam and columns), openings, etc. involved in different experimental campaigns. Moreover, the experimental campaigns involving the study of the effect of plaster and the new infill types have been indicated. Due to the high number of tests, the description of each of them is lengthy and is avoided here, although it could be very insightful. In brief, the properties of masonry infill walls, frames and the loading types involved in different experimental campaigns have been summarised in the following subsections.

Table 1. Overview of OOP experimental studies on infill walls

S.N.	Experimental Study	Scale	Frame	Type	No. of tests	Masonry unit	Hole direction	SR h/t	AR l/h	Loading	IP load	OOP load	Vertical load	Gaps with Beam	Gaps with column	Opening
1	Moghaddam et al. (1988)	<1	Steel	IF	4	SCB	NA (S)	12, 13.9	1.3, 1.4	IP, OOP		D	+	-	-	-
2	Dawe and Seah (1989)	1:1	Steel	IF	9	HCB	V	14.7, 20, 31.1	1.3	OOP		M (AB)	-	- , +	-	- , +
3	Frederiksen (1992)	1:1.36	Steel	IF	16	SCB	NA (S)	26.2	1.2	OOP		M (AB)	-	-	-	-
4	Henderson et al. (1993)	1:1	Steel	IF	2	HCT	H	22.6	1.2	IP, OOP+IP		C (ISD)	-	-	-	-
5	Fowler (1994)	1:1	Steel	IF	20	HCBR	H	11.2	1.5	IP, OOP+IP	D	D	-	-	-	-
6	Angel (1994)	1:1	RC	IF	22	SCB, HCB	NA (S), V	8.7, 11.4, 16.5, 17.7, 34.1	1.5	IP, OOP, IP+OOP	C	M (AB)	- , +	-	-	-
7	Klingner et al. (1996)	1:2	RC	IF	58	SCB	NA (S)	18.4	1.5	IP+OOP, OOP, IP	D	D	+	-	-	-
8	Fardis et al. (1999)	1:1	RC	IF	2	HCBR	NK	21.7, 31.2	1.2	IP / OOP	D	D	+	-	-	-
9	Flanagan and Bennett (1999b)	1:1	Steel	IF	9	HCBL	H	6.8, 11.2, 22.4	1.0	IP, IP+OOP, OOP, OOP+IP, IP / OOP	C	LUR (AB) C (ISD	-	-	-	-
10	Calvi and Bolognini (2001)	1:1	RC	IF	11	HCBL	H	20.4	1.5	OOP, IP+OOP	C	M (PL)	+	-	-	-
11	Zarnic et al. (2001)	1:4	RC	IF	2	SCB	NA (S)	18.6	1.2, 2.3	IP / OOP	D	D	+	-	-	-
12	Tu et al. (2007)	1:1	RC	CM	2	SCB	NA (S)	NK	NK	OOP		M (ISD)	+	-	-	-
13	Corte et al. (2008)	1:1	RC	IF	2	HCT, HCB	NK	NK	NK	OOP		C (ISD)	+	-	-	-
14	Tu et al. (2010)	1:1	RC	IF CM	28	SCB	NA (S)	14.4, 29.5	1.0	OOP		D	+	-	-	-
15	Komaraneni et al. (2011)	1:2	RC	IF, CM	3	SCB	NA (S)	10.8, 21.7	1.8	OOP+IP	C	D	+	-	-	-
16	Liu et al. (2011)	1:3	CES	IF	2	SCB	NA (S)	15.80	2.0	OOP		D	-	- , +	-	-
17	Lunn and Rizkala (2011)	1:1	RC	IF	18	SCBR	NA (S)	NK	1., 1.2, 1.6	OOP		M (AB)	-	-	-	-
18	Pereira et al. (2011) ##	2:3	RC	IF	7	HCBR	H	10, 11.3	2.0	IP+OOP	C	C (AB)	+	-	-	-
19	Rabinovitch and Madah (2011)	1:1	RC	IF	2	HCB	V	10.5, 21.1	0.6	OOP		D	+	-	+	-
20	Varela-Rivera et al. (2011)	1:1	RC	CM	6	HCBR	V	11.7	2.0	OOP		M (AB)	-	-	-	-
21	Varela-Rivera et al. (2012a)	1:1	RC	CM	6	HCB	V	18.1, 19.2, 22.7, 24	1, 1.1, 1.3, 1.35	OOP		M (AB)	-	-	-	-
22	Varela-Rivera et al. (2012b)	1:1	RC	CM	3	HCB	V	18.1, 19.2, 24	1.3, 1.3	OOP		M (AB)	- , +	-	-	-
23	Da Porto et al. (2013)) ##	1:1	RC	IF	7	HCBR	V	8.8, 22	1.6	IP+OOP	C	M (PL)	+	-	-	-
24	Hak et al. (2014)	1:1	RC	IF	5	HCBR	V	8.43	0.5, 1.4	IP+OOP, OOP	C	M (PL)	+	-	- , +	-
25	Ingham et al. (2014)	1:1	RC, CES	IF	21	HCBR	V	21, 22, 25, 27, 35, 40	.3, .4,.5,.8, .9,1.1,1.2,1.3	OOP		LUR(AB)	+	-	- , +	-
26	Da Porto et al. (2015)) ##	1:1	RC	IF	8	HCBR	H	17.7	1.6	IP+OOP	C	M (PL)	+	-	-	-
27	Petrus et al. (2015) **	1:1	Steel	IF	5	HCBL	V	14.0	0.8	OOP		C (PL)	-	-	+	-
28	Preti et al. (2015) **	1:1	Steel	IF	2	HCBR	V	12.9	1.2	IP+OOP	C	LUR (PL)	+	+	-	- , +
29	Akhoundi et al. (2016)	1:2	RC	IF	3	HCBR	H	20.4	1.5	OOP		LUR (AB)	+	- , +	-	- , +
30	Furtado et al. (2016)	1:1	RC	IF	3	HCBR	H	15.3	1.8	IP+OOP, OOP	C	M (AB), LUR (AB)	+ - , +	-	-	-
31	Misir et al. (2016)	1:1	RC	IF	5	HPB, HCBR, SCBL	V, H, NA (S)	7.4, 8.7, 9.1, 13.33	1.6	IP / OOP	C	M (PL)	+	-	-	-

Table 1. Continue….

S.N.	Experimental Study	Scale	Frame	Type	No. of tests	Masonry unit	Hole direction	SR h/t	AR l/h	Loading	IP load	OOP load	Vertical load	Gaps with Beam	Gaps with column	Opening
32	Moşoarcă et al. (2016) **	1:1	Steel	IF	2	HCBL	V	14	0.8	OOP		C (PL)	-	-	+	-
33	Moreno-Herera et al. (2016)	1:1	RC	CM	8	HCB, HCBR, SCB	V, NA (S)	23, 24.2, 24.4	1.1, 1.4	OOP		M (AB)	+	-	-	-
34	Silva et al. (2016) **	2:3	RC	IF	4	HCBR	V	16.3	1.5	IP, OOP	C	LUR (AB)	+	-	-	-
35	Singhal and Rai (2016)	1:2	RC	IF, CM	8	SCB	NA (S)	22.8	0.8	OOP+IP	C	D	+	-	-	- , +
36	Tondelli et al. (2016)	1:2	RC	IF	1	HCBR	NK	14.7	1.1	IP, OOP	D	D	+	-	-	-
37	Verlato et al. (2016)	1:1	RC	IF	5	HCBR	V	9.1	0.5, 1.5	OOP, IP+OOP	C	LUR (PL)	+	-	-	-
38	Spesdar (2017)	1:2	RC	IF	4	HCB	V	10.90	1.4	OOP, IP+OOP, OOP+IP+OOP	M	M (AB)	-	-	-	- , +
39	Wang (2017)	1:2	RC, Steel	IF	5	HCB	V	10.9	1.4	IP+OOP, OOP	M	M (AB)	-	- , +	- , +	- , +
40	Di Domenico et al. (2018)	2:3	RC	IF	3	HCBR	H	22.8	1.3	OOP		M (PL)	-	- , +	- , +	-
41	Onat et al. (2018)	1:1	RC	IF	2	HCBR	H	10.2	2.5	IP / OOP	D	D	+	-	-	-
42	Palieraki et al. (2018)	1:1	RC	IF	2	HCBR	H	25.9	1.3	IP, OOP+IP	C	LUR (PL)	-	-	-	-
43	Ricci et al. (2018a)	2:3	RC	IF	4	HCBR	H	22.8	1.3	IP+OOP, OOP	C	M (PL))	-	-	-	-
44	Ricci et al.(2018b)	2:3	RC	IF	4	HCBR	H	15.2,22.8	1.3	IP+OOP, OOP	C	M (PL)	-	-	-	-
45	Vailati et al. (2018) **	1:1	RC	IF	3	HCBL	V	8	1.7	OOP		LUR (AB)	-	-	-	-
46	Butenweg et al. (2019)	1:1	RC	IF	4	HCBR	V	6.9	1.1	OOP, IP+OOP+IP, IP/OOP	C	CP (AB), LUR (AB)	+	-	- , +	-
47	De Risi et al. (2019)	2:3	RC	IF	4	HCBR	H	22.8	1.0	IP+OOP, OOP	C	M (PL)	-	-	-	-
48	Di Domenico et al. (2019a)	2:3	RC	IF	4	HCBR	H	15.2, 22.8	1.3	OOP		M (PL)	-	- , +	- , +	-
49	Koutas and Bournas (2019)	1:2	RC	IF	6	SCB	NA (S)	8.9, 19.2	1.4	OOP		M (PL)	-	-	-	-
50	Pantò et al. (2019)	2:3	RC	IF	2	HCBR	V	11.6, 16.3	1.5	OOP		LUR(AB)	+	-	-	-
51	Sagar et al. (2019)	1:2	RC	IF	6	SCB	NA (S)	17.10	1.8	OOP+IP	C	D	+	-	-	-
52	Akhoundi et al. (2020)	1:2	RC	IF	3	HCBR	H	20.4	1.5	IP+OOP	C	LUR (AB)	+	- , +	-	- , +
53	Da Porto et al. (2020)	1:1	RC	IF	5	HCBR	V	8.8	1.6	OOP, IP+OOP	C	M (PL)	+	-	-	- , +
54	Furtado et al. (2020)	1:1	RC	IF	2	HCBR	H	15.30	1.8	OOP		LUR (AB)	+	-	-	-
55	Milanesi et al. (2020) **	1:1	RC	IF	2	HCBR	V	8.43	0.5, 1.4	IP+OOP	C	D	+	-	-	- , +
56	Wu et al. (2020)	1:1	RC	IF	4	HCBR	H	7.1	1.1	OOP		D	-	-	-	-
57	Anić et al. (2021)	1:2.5	RC	IF	6	HCBR	V	22.8	1.4	OOP		LUR (ISD)	-	-	-	- , +
58	Di Domenico et al. (2021)	1:1	RC	IF	3	HCBR	H	15.3	1.0	OOP, IP+OOP	C	M (PL)	-	-	-	-

Note: ** indicates the experiment on new infill types as mentioned in the text, ## indicates experiment where the effect of plaster is investigated
RC = Reinforced concrete, CES = concrete encased steel; IF = Infill Wall, CM = Confined Masonry Wall, SR = Slenderness ratio, AR = Aspect ratio
HCB = Hollow concrete block, HCBR = Hollow clay brick, HCT = Hollow clay tile, SCB = Solid clay brick, SCBL = Solid concrete block, HPB = Hollow pumice block
H = Horizontal, V= Vertical, NA = Not Applicable, S = Solid, NK =Not Known, + = exist, - = does not exist
IP = IP load only, OOP = OOP load only, IP+OOP = IP load followed by OOP load, OOP + IP = OOP load followed by IP load, IP+OOP+IP = IP load followed by OOP load and IP load again, OOP+IP+OOP = OOP load followed by IP load and OOP load again, IP / OOP = simultaneously acting IP and OOP load, LUR = Load-unload-reload (unidirectional cyclic loading), D = Dynamic (shake table), M= monotonic, C= Cyclic, ISD = Inter-storey drift, CP = constant pressure, PL = Point load, AB = Airbag

2.1 Variation of frame and infill properties

From a detailed study of the experimental campaigns mentioned above, it was found that most of the tests were conducted on single-storey single-frame specimens. This is related to the financial aspects of the tests and limitations in the lab facilities. Some tests refer to multi-storey frame structures and very few experimental campaigns were conducted in real buildings (Tu et al. 2007; Corte et al. 2008), while Ingham et al. (2014) only tested infill walls at building sites. In some studies, 2 single-frame - single-storey infilled structures with a RC slab were used to perform OOP tests (Fowler 1994; Klingner et al. 1996; Tu et al. 2010). The majority of the experimental campaigns (i.e. 47) regarded infills in reinforced concrete frames, while some of them (i.e. 11) involved infills in steel frames (Fig 1a). Most of the experimental campaigns (i.e. 34) adopted full-scale infilled frames, while 10 of them used half-scaled infilled frames and few others used 2/3 scaled infilled frames (Fig 1b). The distribution of the types of frames and the scale of infilled frames used in different experimental campaigns is described by the bar charts in Fig 1a-b.

Clay masonry units were commonly utilized as a building material for infill walls or confined masonry wall specimens. Out of 58 experimental campaigns, 51 were conducted on masonry made with clay bricks or blocks, and only in 10 experimental campaigns, masonry was made with concrete masonry units (Fig 2a) (in some experimental campaigns clay units and concrete units were used alternatively). In the majority of the experimental campaigns (i.e. 46), infills made with hollow masonry units were used and solid masonry units were adopted in 15 of them (Fig 2b). For infills with hollow masonry units, the two cases of holes laying either in horizontal or vertical direction, representing the construction practices, were investigated (Fig 2c). Few experimental campaigns have involved infill walls made of both solid and hollow masonry units (Angel 1994;

Misir et al. 2016; Moreno-Herera et al. 2016). Furtado et al. (2018) found that OOP strength of infill walls reduced when the percentage of the void in hollow masonry units increased.

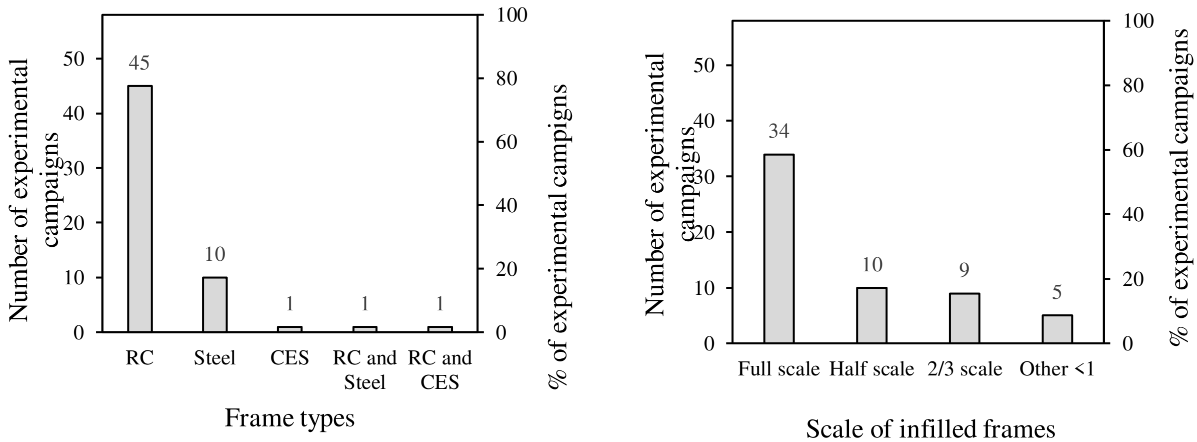

a) b)

Note: CES = Concrete Encased Steel

Fig 1. Properties of infilled frame specimens in different experimental campaigns: a) Types of frames, and b) scale of specimens

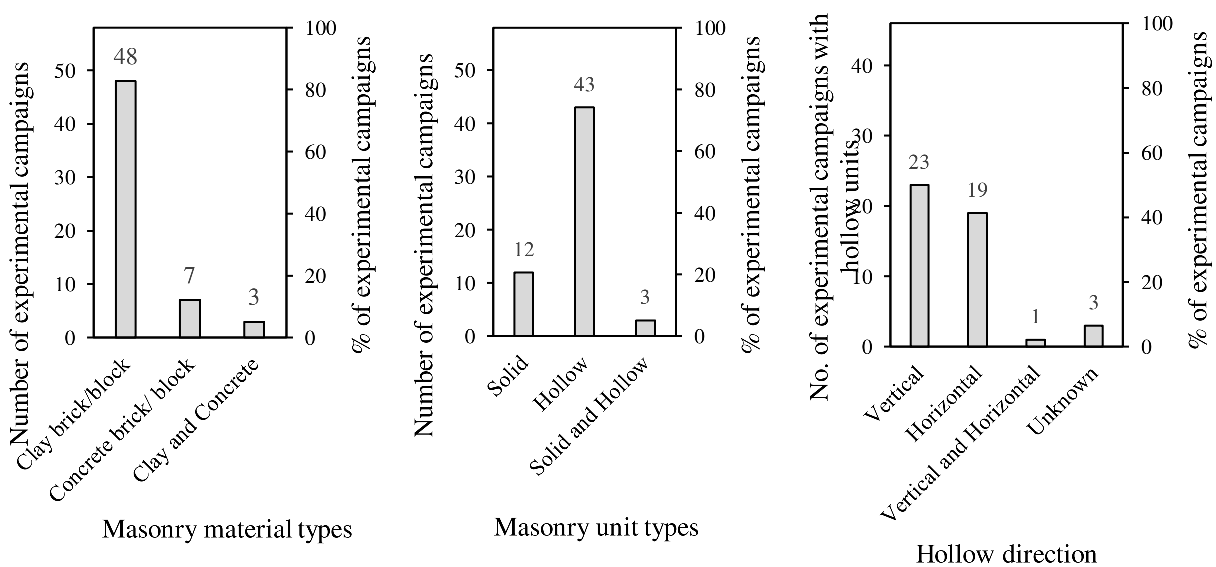

a) b) c)

Fig 2. Characteristics of infills in different experimental campaigns: a) material types, b) unit types, and c) direction of holes of units

The geometrical properties of the URM infills used in different experimental campaigns also have high variations. The tested infills had a slenderness ratio in the range of 6.8 to 34.2, while the infills' aspect ratio ranged from 0.5 to 2.5 as shown in Table 1. The distribution of the aspect ratio of the experimented infills or confined masonry specimens is also shown in Fig 3. The length of the infill specimens tested is generally greater than the height. Most of the experimental campaigns involves specimens with an aspect ratio in the range of 1.0 - 1.6. The distribution of the slenderness ratio of the specimens used in the experimental campaigns is shown in Fig 4. In detail, the range of thickness of infill wall specimens varied from 30 mm to 365 mm (Fig 5).

It has to be noted that in Fig 3 the total number of experimental campaigns is more than 58. It is because, in few experimental campaigns, infill specimens with more than one aspect ratio were tested (the same applies to the distribution of slenderness ratio in Fig 4 and the distribution of thickness in Fig. 5 - details in Table 1). Therefore, those experimental campaigns were counted more than one time.

From Fig 5, it can be observed that in 4 cases infill thicknesses even below 50 mm have been used. However, only one of them (Angel 1994) refers to full-scale tests while 3 others (Frederiksen 1992; Klingner et al. 1996; Zarnic et al. 2001) used small-scaled specimens. The same figure also shows that there are not many experimental campaigns with thick infill walls (200 mm or higher) while 5 of them still belong to the category of innovative infill types, characterized by different construction techniques as discussed at the beginning of section 2 (these innovative infills, provided with sliding joints or enclosure systems for reinforcement, partitioned, etc., cannot be directly compared to URM infill walls used in construction practices). This highlights a serious lack of tests for understanding the OOP capacity of thick infill walls.

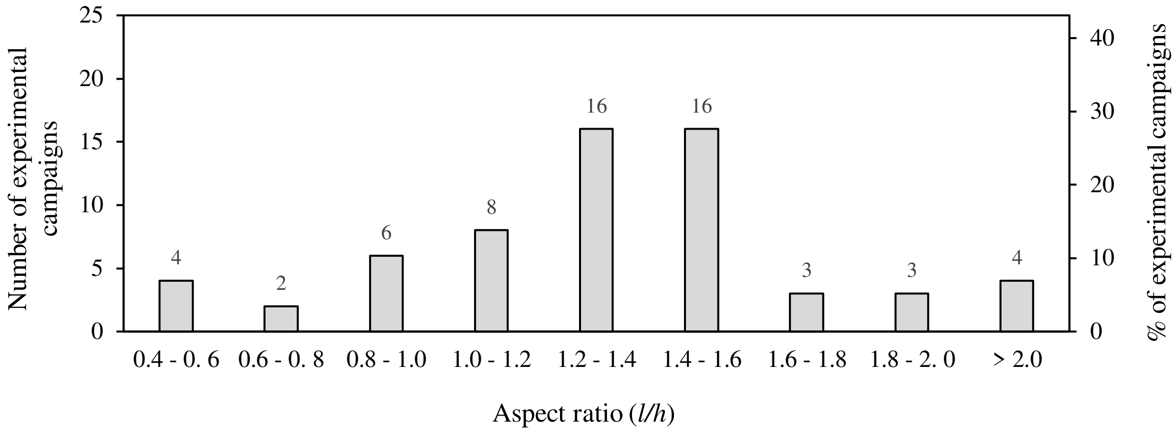

Fig 3. Distribution of the experimented infill specimens as per their aspect ratio

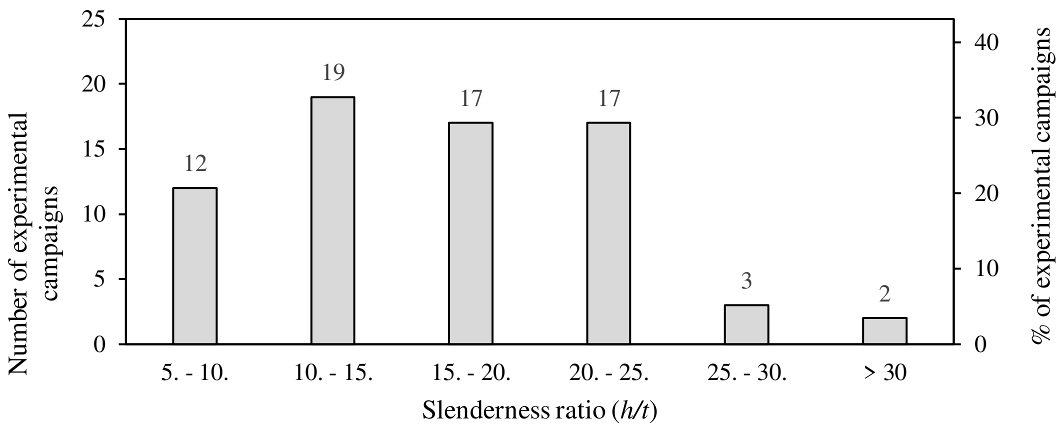

Fig 4. Distribution of the experimented infill specimens as per their slenderness ratio

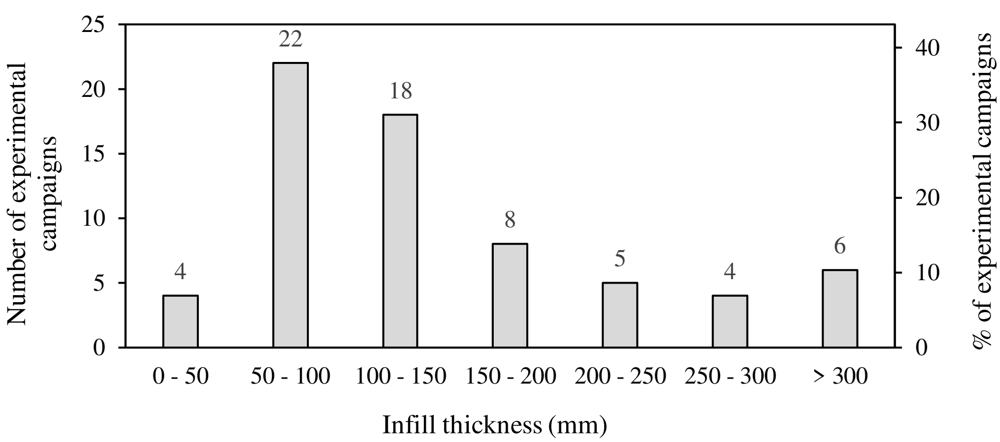

Fig 5. Distribution of thickness of infills used in the experimented specimens

The compressive strength of the masonry in infill wall specimens tested in different experimental campaigns varied from 0.5 to 35 MPa. In some of the experimental campaigns, such mechanical property of masonry is not known, and in the most of the cases, properties of the masonry units and mortar are not provided by the authors. Further, in the case of infill walls with hollow masonry units, typically, the compressive strength of the masonry is different in the directions parallel and perpendicular to the holes in the unit due to the different strengths of the units in these two directions. However, different experimental campaigns report the strength of masonry only in one direction, that is the direction of the gravity loads.

Fig 6 summarizes the range of compressive strength of the infill specimens made with solid units used in different experimental campaigns. The figure shows that the number of experimental campaigns is very low in each range of compressive strengths. In some range of strengths, no infill specimens with solid masonry units were tested. Similarly, Fig 7 shows the variation of the compressive strength of infill specimens made with hollow units in the directions parallel and perpendicular to the unit holes (the strengths in the horizontal and vertical directions refer to the same experimental campaigns; in some cases, the strength perpendicular to holes, when the holes are in the gravity direction, is not provided by the authors). The majority of experimental campaigns used infill specimens with low compressive strength (0 to 4 MPa). Figs 6 and 7 highlight that experimental investigations on different ranges of infill masonry's strength are lacking.

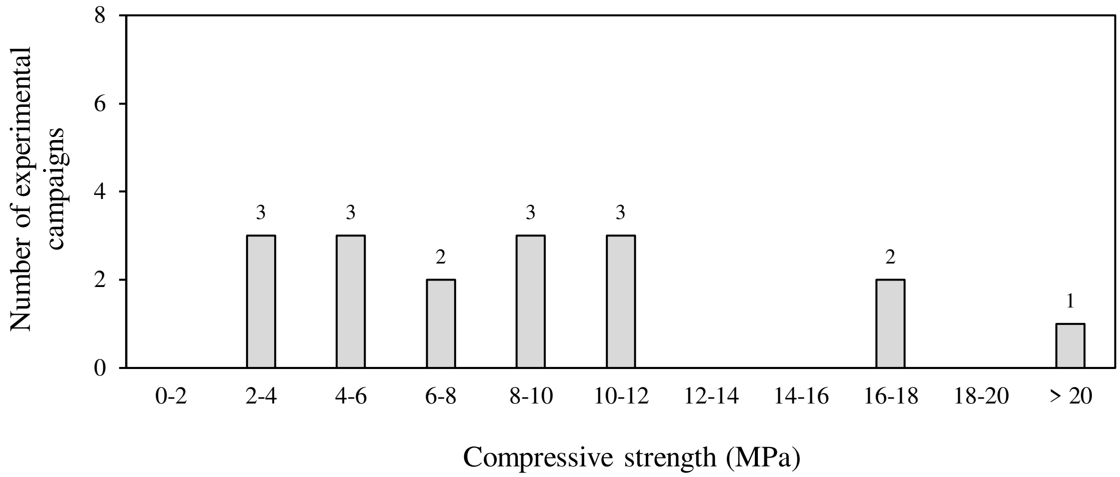

Fig 6. Compressive strength of masonry with solid units in different experimental campaigns

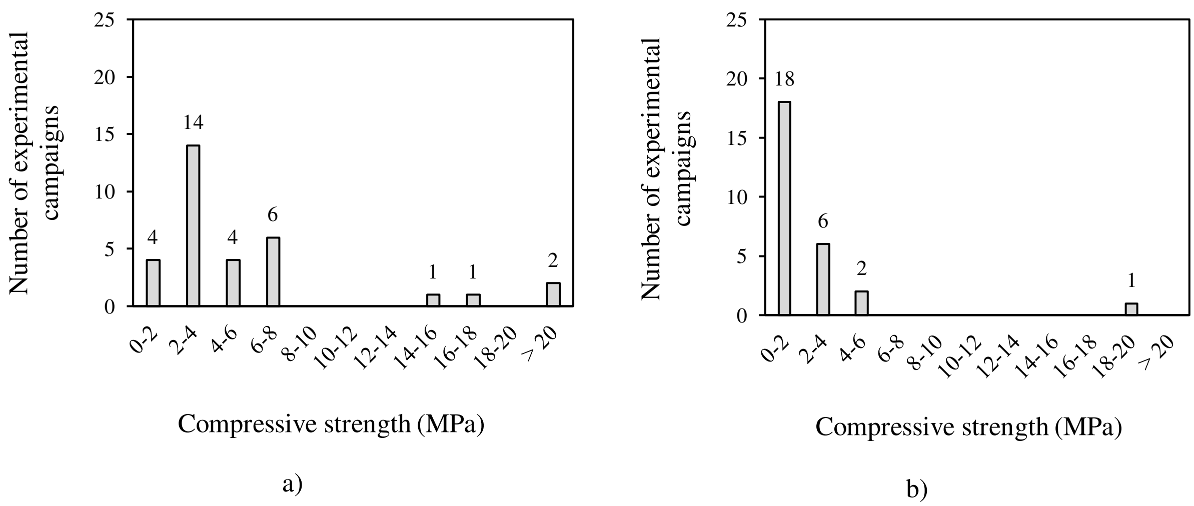

Fig 7. Compressive strength of masonry in the experimental campaigns involving masonry infills with hollow units: a) parallel to hole; b) perpendicular to hole

2.2 Variation of loads and loading methods

Out of 58 experimental campaigns, in 27, infill specimens were tested only with OOP loads, whereas in 15, the infill specimens were tested with combined IP and OOP loads applied sequentially or simultaneously. In the remaining 16 experimental campaigns, infilled specimens were tested both with OOP loads and combined IP and OOP loads (Fig 8a). The majority of the experimental campaigns (i.e. 43 which is almost 75%) were conducted using quasi-static loading methods while the other 15 were performed under dynamic settings with the use of a shake table (Fig 8b). The decision to use a quasi-static or dynamic approach is largely affected by the cost of experimentation and the objective of the test. For example, to understand the maximum OOP force that an infill can sustain, loading under static conditions is more appropriate. Nevertheless, dynamic excitations by the shaking table best represent the earthquake effect.

Most of the quasi-static tests (i.e 39) were performed by applying an OOP load on the infill wall directly. This method is also known as the inertial method of loading (Anić et al. 2019). In such loadings, either uniform pressure was maintained all over the infill area by using an airbag, or the infills were pushed at some local points by using concentrated loads (22 experimental campaigns - airbags, 17 experimental campaigns - point loads) as shown in Fig 8c. Very few experimental campaigns used inter-storey drift load, either monotonic or cyclic, applied on the frame (e.g. Henderson et al. 1993; Flanagan and Bennett 1999b; Tu et al. 2007, Corte et al. 2008; Anić et al. 2021). In the inertial method of loading, damage primarily occurs to infill walls, but in the case of an inter-storey drift load, the damage is concentrated more in the frames.

The difference in the load shape used for loading an infill (point loads or uniform pressure) can influence the OOP capacity of the infill (Di Domenico et al. 2018; Di Domenico et al. 2019b). In the inertial method of loading, normally three different approaches were found to be adopted: i) application of monotonically increasing force or pressure; ii) application of unidirectional cyclic (load-unload- reload cycles) of force or pressure; and iii) application of cyclic force or pressure. Furtado et al. (2016) experimented using both (i) and (ii) types of loading. Repeatedly applied unidirectional loading is a simplified representation of cyclic loading (distribution of types (i), (ii) and (iii) is shown in Fig 8d).

In dynamic test conditions, very few experimental campaigns used simultaneously applied IP and OOP shaking (e.g. Fardis et al. 1999; Zarnic et al. 2001; Onat et al. 2018), and in other cases loading was an unidirectional shaking. For IP testing, monotonic or cyclic drift loads were applied at the frame top in quasi-static settings, or else a shake table was used. In the majority of the cases, cyclic IP loads were adopted (24 experimental campaigns) and monotonic IP loads were rarely used (only in 2 experimental campaigns). The use of different loading methods for IP testing of infilled frames can be seen in Fig 8e.

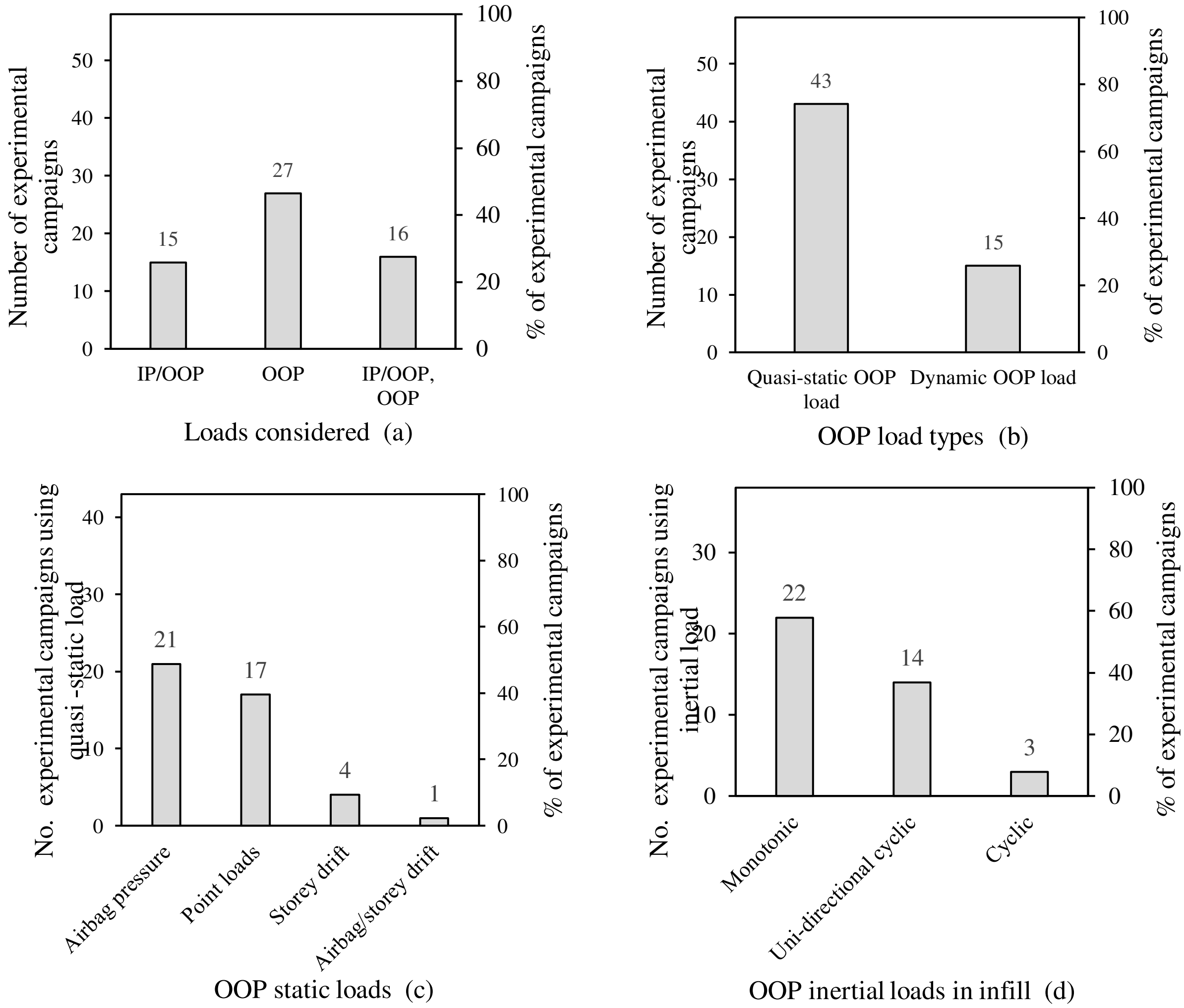

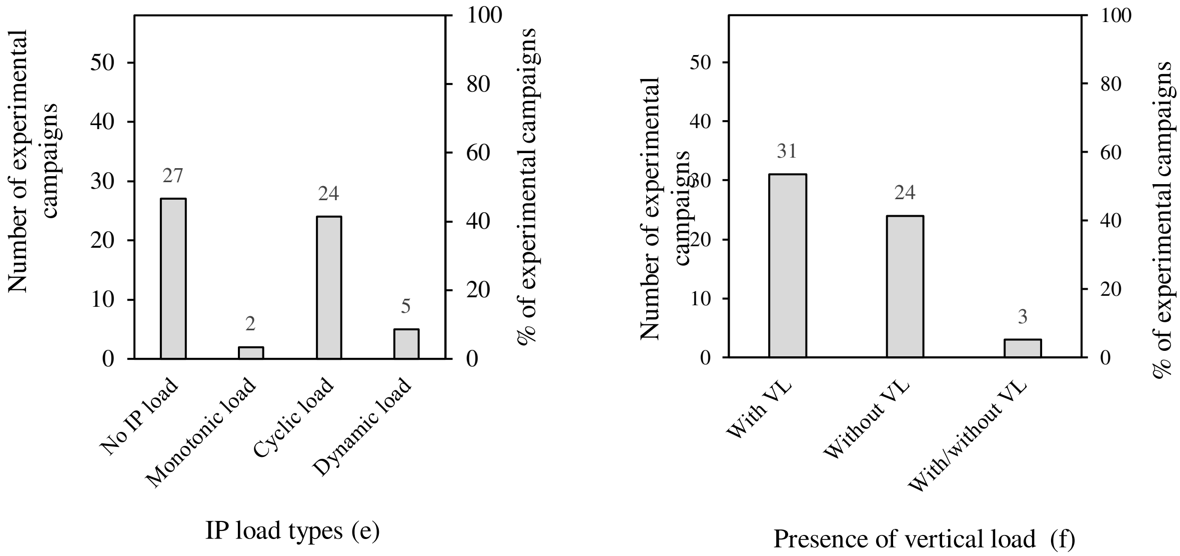

Fig 8. Summary of types of loading applied to specimens: a) load used, b) OOP loads types, c) quasi-static OOP loads, d) types of inertial loads, e) IP loads, and f) use of vertical load (VL)

Tests were carried out either in the presence or absence of vertical load. Vertical loads are used to simulate the gravity load coming from the upper floors. Vertical loads were used in 34 experimental campaigns and among them, 3 also involved specimens without gravity load (as shown in Fig 8f). In such experimental campaigns, 19 of them (approximately 55%) applied gravity loads directly over the columns and others applied gravity loads on the beam or RC slab.

Variations like mechanical properties of masonry, dimensions of infill walls (slenderness ratio, aspect ratio), tests on IP damaged or undamaged specimens, etc. resulted in different OOP capacities. For a quick look, the plot of the OOP capacities of infilled or confined masonry specimens against the slenderness ratio is shown in Fig 9. 120 specimens have been included in the plot. The effect of the slenderness ratio is evident, the higher the slenderness ratio the lower the capacity. However, it has not to be forgotten that there are influences of several other factors that are dealt with in detail in the next sections.

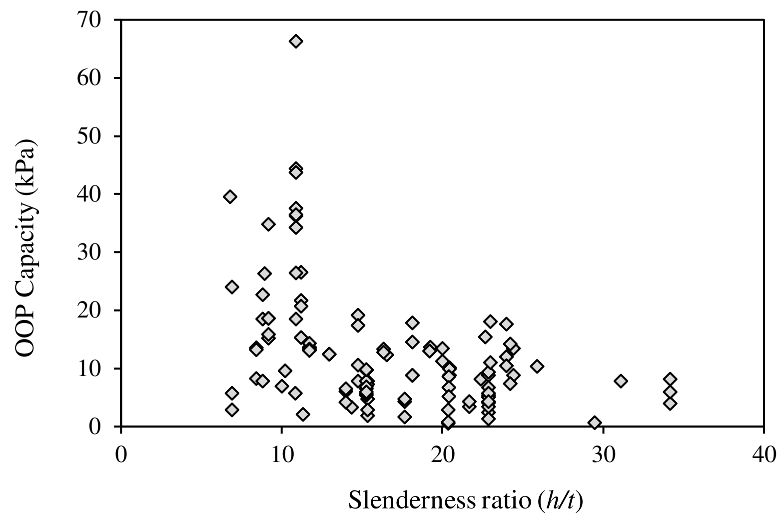

Fig 9.Experimental OOP capacities of the infilled/ confined masonry specimens versus slenderness ratio

3. OOP infill capacity: discussion of the results from the experimental studies

In this section, results from various tests are compared. To compare the OOP capacities of masonry infills with different characteristics, OOP capacity has been expressed in kiloPascal (kPa). For all OOP load-displacement plots, the displacement at the centre of infill has been used. OOP displacement is also expressed in terms of OOP drift (%) with respect to half the height of the infill wall.

3.1 Effect of slenderness ratio

OOP capacity is connected with the arching action and experimental campaigns have demonstrated that the arching mechanism is very effective in thick infills. The arching action differs depending upon the slenderness ratios in the vertical and horizontal directions. According to Angel (1994), arching occurs when the slenderness is less than a limit known as the critical slenderness ratio. When the slenderness ratio of the infill wall is higher than the critical slenderness ratio, snapping failure occurs. Dawe and Seah (1989) investigated the influence of the slenderness ratio (*h/t)* on the OOP response of masonry infill walls with the same mechanical characteristics. From their results, it was found that the masonry infill wall specimens called WE2, WE4 and WE5 having thicknesses 190 mm (*h/t* =14.7), 140 mm (*h/t* =20) and 90 mm (*h/t* =31) respectively obtained a peak OOP capacity of 19.2 kPa, 11.2 kPa, and 7.8 kPa.

Similarly, Angel's (1994) specimens 3, 6 and 8 with thicknesses of 47.6 mm (*h/t* =34), 98.4 mm (*h/t* =14.7) and 187.3 mm (*h/t* =8.7) respectively made of the same material (brick and lime mortar) but with different mechanical properties (elastic modulus and compressive strength) exhibited an OOP strength of 6 kPa, 12.4 kPa, and 32.1* kPa (* indicates that tests were stopped due to the limited capacity of the testing equipment). The high strength in the case of thick infills was attributed to higher arching action. Flanagan and Bennett (1999b) also obtained similar results. Specimens 25, 18 and 22 having thicknesses 100 mm (*h/t* =22.4), 200 mm (*h/t* =11.2), and 330 mm (*h/t* =6.8) respectively, and similar mechanical properties showed OOP strengths of 8.1 kPa, 26.6 kPa and 39.5 kPa respectively. However, experimental tests carried out by Varela-Rivera et al. (2012a) did not show significant changes in OOP strength with a small difference in slenderness ratio, confined masonry wall E2 (with a thickness of 150 mm i.e. *h/t* =19.2) and E3 (with a thickness of 120 mm i.e. *h/t* =24) with a similar compressive strength bounded with confining elements having almost equal IP stiffness demonstrated the strength of 13 kPa and 12 kPa respectively.

Koutas and Bournas (2019) also found that the OOP capacity of the thick infill specimen D_CON (thickness of 140 mm or *h/t* =8.9) was almost two times that of the thin infill specimen S_CON (thickness of 65 mm or *h/t* =19.2). Likewise, experimental investigations by Ricci et al. (2018a, 2018b) on infills's thicknesses 80 mm (*h/t* =22.8) and 120 mm (*h/t* =15.2) demonstrated that the OOP capacity for a thick infill was double of that of a thin infill wall (results in Fig 10). It is worth pointing out that the two infills had similar mechanical properties. Shake table tests by Tu et al.

(2010) also showed that the OOP resistance was increased significantly when the thickness of the confined masonry panel was doubled (case of *h/t* =29.5 and 14.4).

Fig 10 highlights the effect of the slenderness ratio in the OOP behaviour of URM infills observed in some experimental studies. It has to be noted that the infill specimens compared in the figure have different masonry strengths (compressive strength was less than 2 MPa in the case of Ricci et al. 2018a and 2018b, while it was about 10 MPa in the case of Koutas and Bournas 2019). These experimental results indicate the strong influence of the slenderness ratio on the OOP capacity of infill walls.

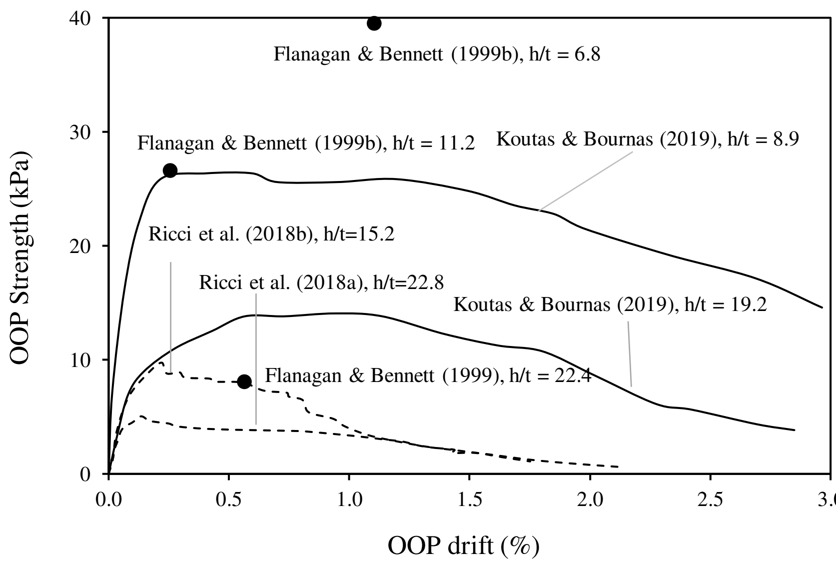

Fig 10. Influence of slenderness ratio (*h/t*) on the OOP capacity of masonry infill wall panels

Although it has been confirmed that OOP strength increases with an increase in the thickness of the infill wall, there are still very few experimental campaigns conducted on thick infill walls as discussed in section 2.1.

3.2 Effect of aspect ratio

De Risi et al. (2019) compared the OOP performance of infill walls having aspect ratio (*l/h*) 1.0 with specimens tested by Ricci et al. (2018a) having aspect ratio 1.28. The thickness of the infill specimens in both tests was 80 mm and the mechanical characteristics (masonry compressive strength and elastic modulus) of the infill walls were similar (slightly higher in the former). OOP capacity of the infilled specimen was lower when the *l/h* value increased (Fig 11). Experimental comparisons by Di Domenico et al. (2019a) and Di Domenico et al. (2021) also showed the higher OOP strength in the case of square infill compared to infill with *l/h* equal to 1.28 for 120 mm thick wall although the compressive strength of masonry was slightly higher in the former case.

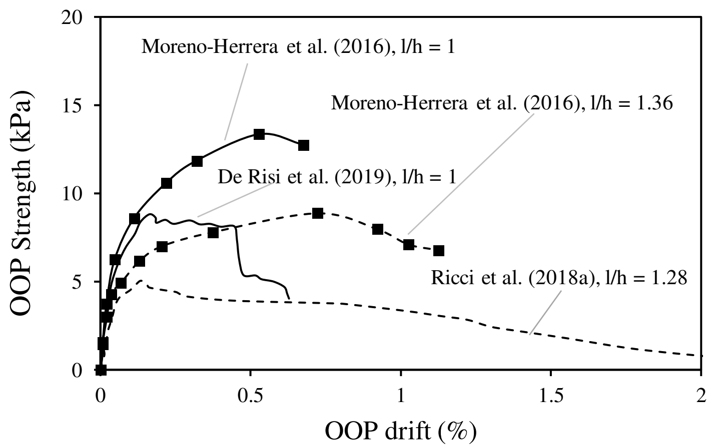

Fig 11. Influence of infill's aspect ratio in the OOP capacity

Moreno-Herera et al. (2016) also observed a reduction of OOP strength and stiffness due to an increase in the aspect ratio (from 1 to 1.36) of the confined masonry walls made of both concrete blocks and clay bricks. Two cases of hollow concrete blocks (particularly specimens W2 and W5) are shown in Fig 11.

Experiment by Varela-Rivera et al. (2012a) also showed a decrease in the OOP capacity of a confined masonry wall with the increase in aspect ratio. In detail, specimen E1 with *l/h* value 1.35 showed OOP strength almost half compared to specimen E5 with *l/h* value 1.08; nonetheless, the confining elements for the latter had slightly higher IP stiffness. Similarly, the experiment of Lunn and Rizkala (2011) also showed the reduction of the OOP strength when the aspect ratio of confined walls with fibre reinforced polymer (FRP) overlaying increased. Thus, the OOP capacity can be expected to be maximum for an infill when its aspect ratio is near to 1.

Fig 12 shows the differences in the cracking pattern of infill walls as observed in the experiment of Moreno-Herera et al. (2016) due to changes in the aspect ratio. It can be observed that the horizontal cracking length at mid-height is longer when there is an increase in the span length.

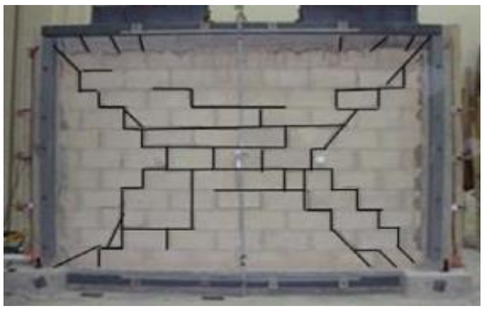

Concret block masonry (*l/h = 1.36)*

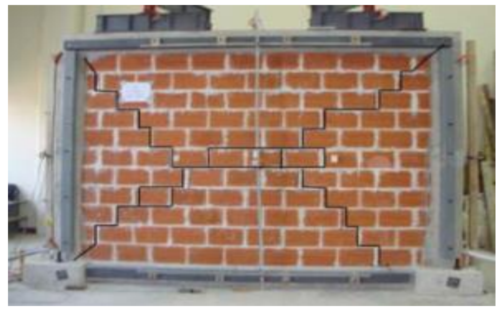

Hollow Clay brick masonry (*l/h = 1.36)*

Concrete block masonry (*l/h = 1.0)*

Hollow Clay brick masonry (*l/h = 1.0)*

Fig 12. Influence of aspect ratio in failure mode of infills due to OOP load (after Moreno-Herrera et al. 2016)

3.3 Effect of IP damage

Several experimental studies have dealt with the OOP behaviour of pre-damaged masonry infill walls (Angel 1994; Flanagan and Bennett 1999b; Calvi and Bolognini 2001; Furtado et al. 2016; Spesdar 2017; Wang 2017; Ricci et al. 2018a, 2018b; De Risi et al. 2019; Akhoundi et al. 2020, Di Domenico et al. 2021). In the experimental campaigns, IP drift load (expressed as inter-storey drift ratio or IDR) applied before the application of OOP load, is commonly taken as a measure of IP damage. The ratio of OOP strength of the IP damaged and undamaged specimens from different experimental campaigns can be viewed in Fig 13. Simply, an increase in the IP damage caused a decrease in OOP strength in every test. But, some specimens with higher IP drift have also shown lower strength reduction when compared to each other. This highlights that the rate of decrease is not only dependent on the amount of prior IP drift.

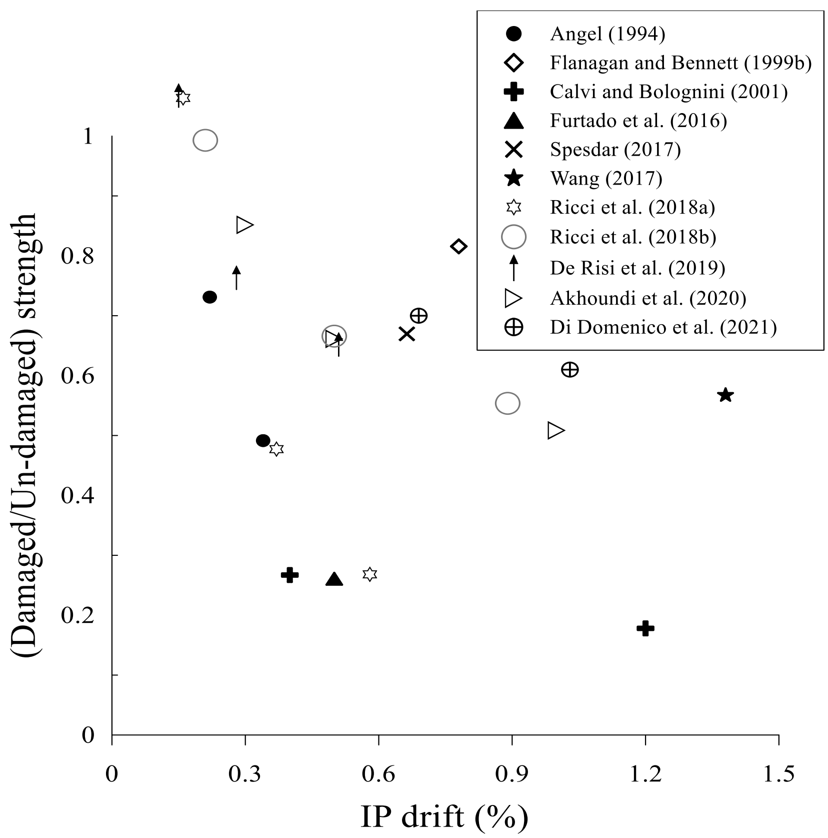

Fig 13. OOP strength reduction observed from experimental studies

In the experimental campaign of Angel (1994), the author experienced a higher reduction of OOP capacity due to increasing IP drift. In particular, specimen 1 without any IP damage (IDR=0%) showed OOP capacity of 8.3 kPa while specimen 3 suffering IP damage (IDR=0.22%) showed a capacity of 5.85 kPa (approximately 70% of specimen 1), and specimen 2 (IDR=0.34%) showed about 4.1 kPa (approximately 50% of specimen 1). Specimens 1, 2 and 3 had the same thickness

(48 mm), but specimen 3 was cast with weak lime mortar while specimen 2 was made of strong N-type (cement, lime, sand) mortar. Specimen 2 had almost double the elastic modulus of specimen 3, although both specimens had similar compressive strength. The higher reduction of strength was due to a very small thickness of infill specimens (h/t = 34). It was strange that specimen 2 which experienced an IP drift only 0.12% higher than that of specimen 3, showed OOP strength reduction by more than 20%, although the former was made with strong mortar (Fig 14). By contrast, an experiment by Flanagan and Bennett (1999b) showed a reduction of only 20% of OOP strength due to 0.78% IP drift. Similarly, the experimental results by Hak et al. (2014) also did not show a major difference between OOP strengths of two infill specimens which were loaded beforehand to an IP drift of 1% and 1.5% (Fig 14). However, degradation of the OOP stiffness was significant (about 40%). In the case of 1.5% drift, IP cracking was spread in the frames while in the case of 1.0% drift, no cracking in the frames was observed. Cracking in the infills, especially in the upper bricks near the top beam, were similar in both cases (slightly more extensive in the case of 1.5% drift). But, the OOP damage was higher in the case of 1% IP drift: extensive damage occurred in the region where the upper right stepwise crack joined the central horizontal crack.

Dynamic tests by Klingner et al. (1996) also revealed a decrease in stiffness by two-thirds of the previously cracked infill due to IP load in comparison to the undamaged specimen. But, Spesdar's (2017) tests indicated a reduction of capacity by only 33% after damage in IP by 0.64% drift. Further tests by Wang (2017) on an infill similar to the one examined by Spesdar (2017) showed a reduction of capacity by 43% after 1.37% IP drift (Fig 14). In these tests, since the IP loads were applied monotonically, the reduction of OOP strength could have been smaller. It could be also because Spesdar‘s (2017) and Wang's (2017) tests were carried out in small-scale specimens, and the slenderness ratio was low (<11). At the same time, their specimens failed in relatively small OOP drift.

Findings by Ricci et al. (2018a, 2018b) also support that the decay of OOP strength can be lower for infills with a low slenderness ratio. In particular, tests on 80 mm thick infill (*h/t*=22.9) indicated a 73% decay while tests on 120 mm (*h/t*=15.2) thick infill specimen showed a reduction by 45% although the latter was damaged in IP by 0.89% and the former was damaged by 0.58% IP drift, despite both type of infills had similar mechanical characteristics of masonry (Fig 14). Experimental results in Di Domenico et al. (2021) further supports this claim.

The results by Calvi and Bolognini (2001) showed a sharp decrease in OOP strength (reduction by approximately 73%) due to a prior IP drift of only 0.45%. A similar result was observed by Furtado et al. (2016): when an infill was OOP loaded only after 0.5% IP drift, the strength reduction was about 75%. Ricci et al. (2018a) also reported an OOP strength reduction of 73% due to IP drift of 0.58% for the case of 80 mm thick slender infills. Interestingly, while testing in IP, Furtado et al. (2016) tested double-leaf infills (150 mm+110 mm) and loaded in OOP only the 150 mm (*h/t*=15.3) thick leaf, and Ricci et al. (2018a) tested the slender 80 mm thick (*h/t*=22.9) infill and used the highest IP drift among the three, but the strength reduction was larger for the former. Although the thickness of infill was the biggest for Furtado et al. (2016) among the three, masonry was very weak (the lowest compressive strength). For Ricci et al (2018a), infill thickness was lower but the masonry was comparatively stronger. This highlights that the decay of OOP strength is significantly influenced by masonry strength. This is supported by the result of Calvi and Bolognini (2001) as well: although the infill thickness of 135 mm (*h/t*=20.3) was used, masonry strength was too low, and only with 0.45% prior IP drift, there was a large reduction in OOP capacity.

The results from Calvi and Bolognini (2001), Ricci et al. (2018b) and De Risi et al. (2019) were similar in the sense that the specimens loaded purely in OOP reached the peak strength within a small OOP displacement (drift) and the capacity dropped quickly afterward. In other experimental campaigns, the OOP strength dropped more gradually for the undamaged specimens. These results also indicate that if the masonry is very weak (too low compressive strength), the OOP strength of the IP-undamaged infill wall can degrade quickly after attaining peak strength (Fig 14).

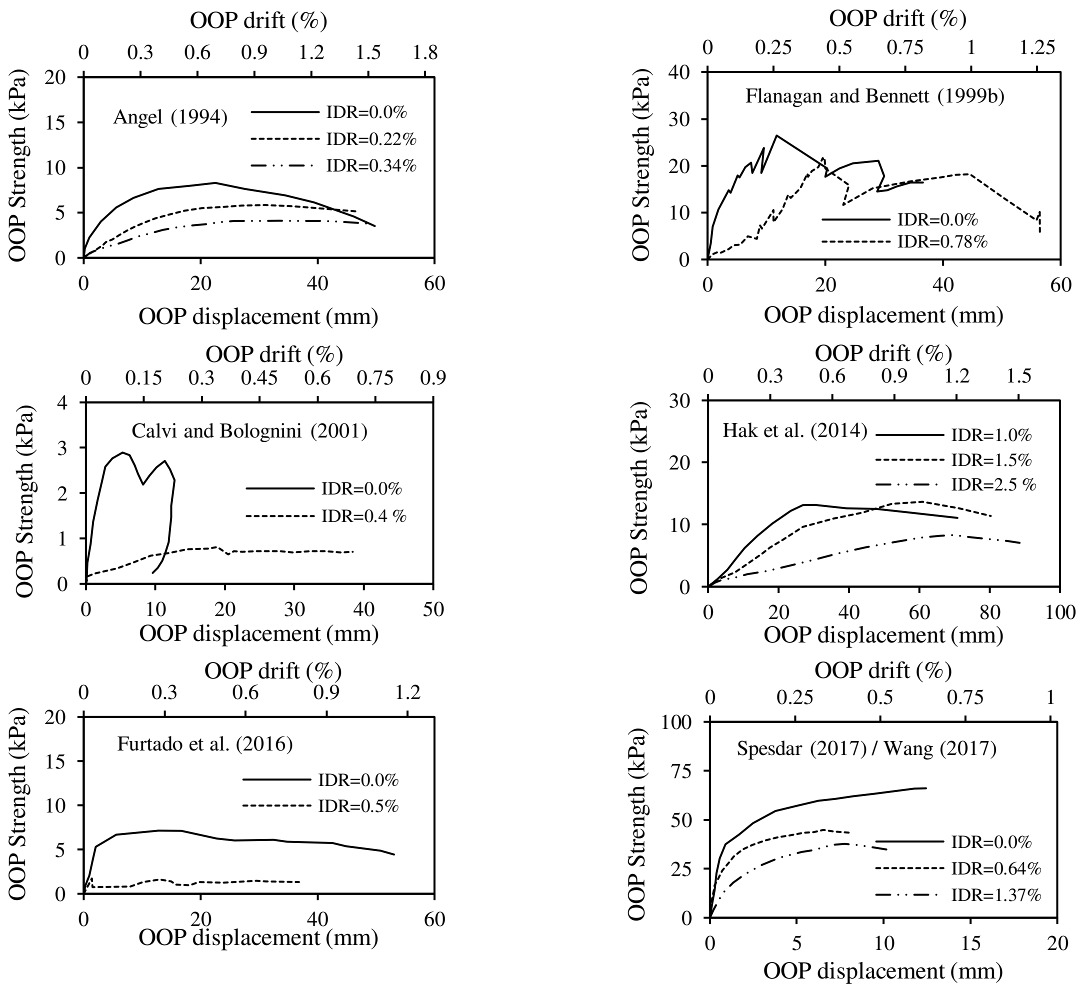

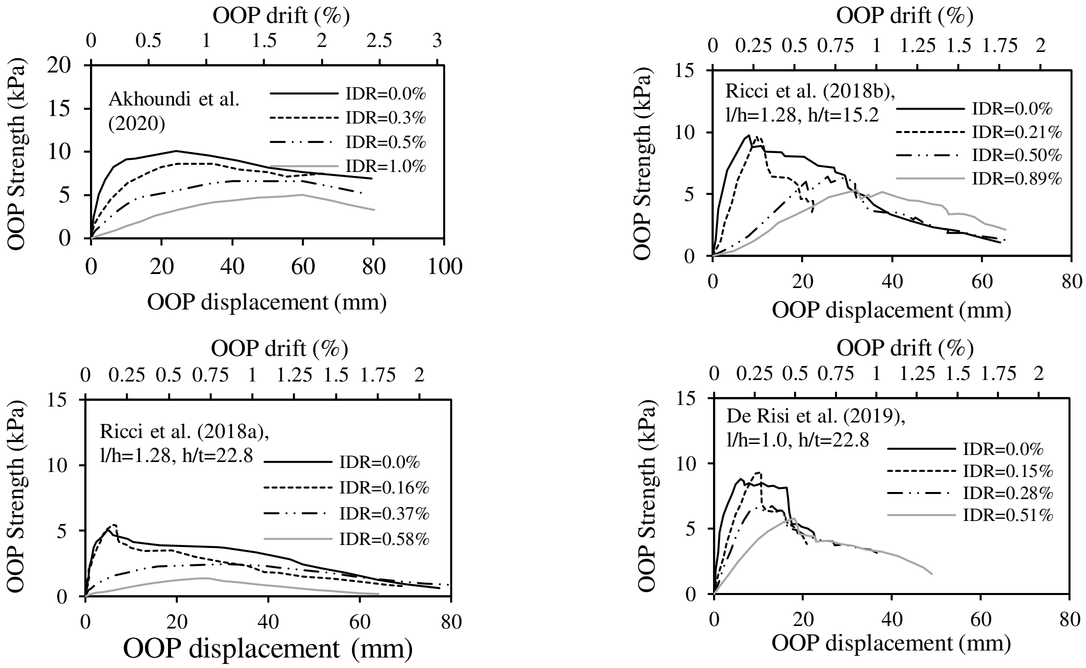

Fig 14. OOP strength – displacement curves according to IP damage level defined by inter-storey drift ratio (IDR)

Unlike OOP strength, the OOP deformation capability seems to be affected differently due to IP damage. In the experimental studies by Calvi and Bolognini (2001), Ricci et al. (2018b) and De Risi et al. (2019), peak strength was achieved at higher drift and the infill specimens failed at large OOP deflection for IP-damaged specimens. This is because the arching effect is delayed due to IP damage. Also, in the experimental studies by Angel (1994), Hak et al. (2014), Spesdar (2017), Wang (2017) and Akhoundi et al. (2020), OOP capacity reduced by almost half (although at different levels of IP drift), but the specimens failed by reaching almost the same OOP deformation for different levels of IP damage considered (Fig 14). This indicates that even if the infills are severely damaged in IP, they can maintain stability in the OOP direction due to the arching.

The above experimental results indicated that the OOP strength reduction depends upon factors that interact with the level of IP damage (IP drift) sustained by the infill wall. The huge variability in the reduction of OOP strength is affected by the nature of IP loads (cyclic or monotonic), masonry strength, infill thickness, etc., interacting with each other. Such dependencies have been highlighted through numerical studies as well (Agnohotri et al. 2013; Wang et al. 2020).

3.4 Effect of boundary conditions

Boundary/restraint conditions between infills and surrounding frame members can vary. Gaps between frame members and infill may arise due to practical necessity or many times because of the nature of the workmanship (Akhoundi et al. 2016). These gaps can reduce the OOP capacity of infill walls.

Dawe and Seah (1989) found a reduction of OOP strength by 45% due to a 5 mm gap between infill and top beam (specimen WE2 vs. WE6). Also, Akhoundi et al. (2016) observed a reduction of the OOP capacity in infill walls by 10% because of a gap with the top beam due to poor workmanship (Fig 15). Furthermore, experimental studies carried out by Spesdar (2017) and Wang (2017) demonstrated that a 10-mm gap between infill and top beam resulted in a higher reduction (72%) of the OOP strength than in the case of 5-mm gaps with the columns that caused only a 45% reduction.

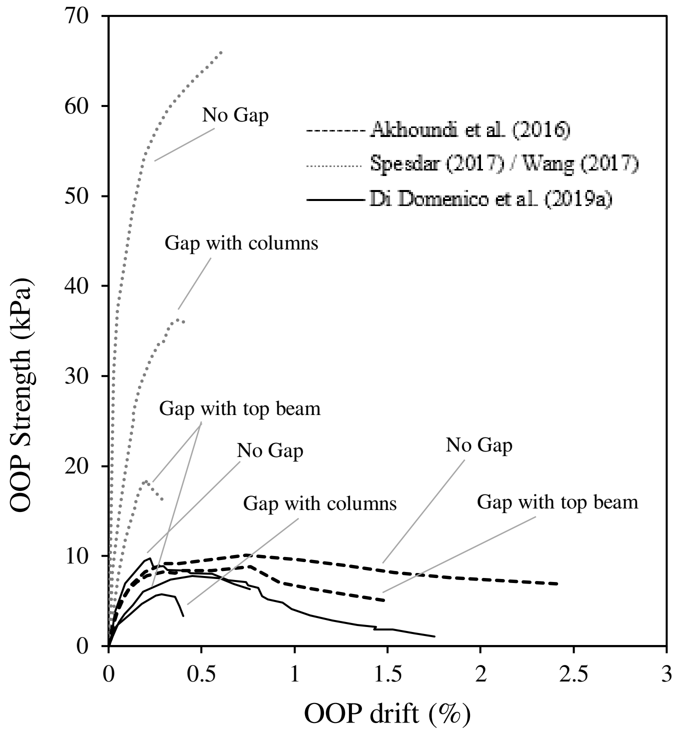

Fig 15. Effect of boundary conditions in the OOP capacity of infill walls

Di Domenico et al. (2018) found contrasting results. According to their findings, the OOP strength of an 80-mm thick infill with no gap was about 5.1 kPa and that with a small gap (i.e. 2 mm) at the top was about 4.1 kPa while the third infill specimen having gaps with columns showed a strength of 3.4 kPa. A small gap at the top of the infill wall only delayed vertical arching but did not eliminate it. Di Domenico et al.'s (2019a) experimental tests on the same thickness infill confirmed that with a larger gap at the top (i.e. 40 mm), vertical arching was not present and capacity was reduced to 4.3 kPa. Further tests by Di Domenico et al. (2019a) on 120 mm thick infill specimens followed a similar strength pattern. The capacity was the highest for an infill with no gap (9.7 kPa), while, for an infill with a 40 mm gap at the top, it was about 7.8 kPa. The capacity was the lowest for an infill with a 30 mm gap with both columns (5.6 kPa) as shown in Fig 15.

The effect of the boundary conditions can also be confirmed from tests on confined masonry walls where the confining elements were built after the masonry wall. The chances of formation of gaps between the wall and frame are less in such constructions. During OOP shake table tests by Tu et al. (2010), normal infill specimens exhibited arching at low motion intensity but separated from the boundary frames at a higher intensity. However, confined walls remained intact even at higher intensity motion.

The reduction of OOP strength due to gaps is influenced by the incapacity of the infill to form arching or due to delayed activation of arching. On one hand, the gap with the beam affects vertical arching and on the other hand, the gaps on the sides affect horizontal arching. Although reduction of strength due to gaps is clear, there is still no consensus about the cases in which gaps with the beam are detrimental compared to gaps with the columns. This can be related to the infill's aspect ratio or compressive strength of masonry in the directions parallel and perpendicular to the holes especially in the case of hollow masonry units, as indicated in Di Domenico et al. (2019a). Wang (2017) laid masonry with holes in the vertical direction while in Di Domenico et al. (2018) and Di Domenico et al. (2019a), masonry was laid with holes in the horizontal direction. Fig 16 shows the influence of gaps on the cracking patterns in masonry infills due to OOP load.

No gap　　　*Top gap*

Study by Akhoundi et al. (2016)

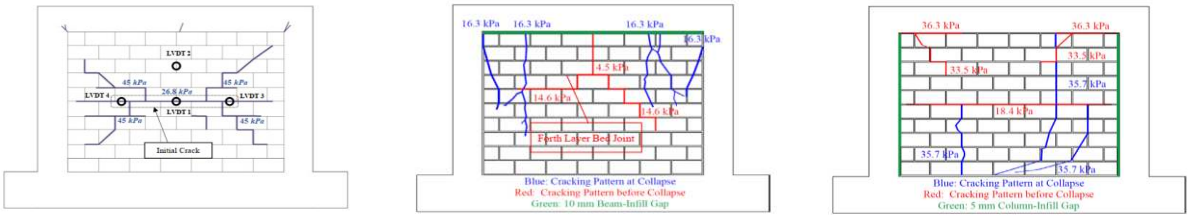

No gap *Top gap* *Side gaps*

Study by Wang (2017)

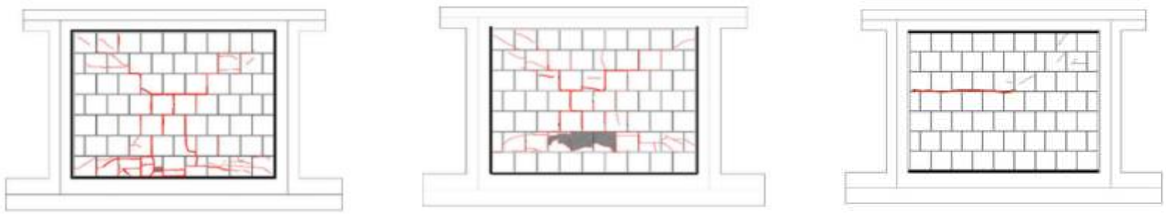

No gap *Top gap* *Side gaps*

Study by Di Domenico et al. (2018)

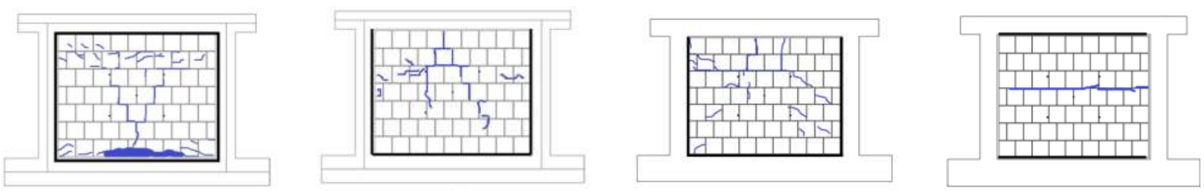

No gap (120 mm infill) *Top gap (80 mm infill)* *Top gap (120 mm infill)* *Side gaps (120 mm infill)*

Study by Di Domenico et al. (2019a)

Fig 16. Influence of gaps in cracking pattern of infill walls developed due to an OOP load

3.5 Effect of openings

Experimental results have shown that OOP strength is not highly influenced by the presence of small openings like doors and windows. Dawe and Seah (1989) experienced a reduction of only 10% of the OOP capacity due to the presence of a central window (specimen WE9) measuring 1.6 m×1.2 m (19% area of infill) in comparison to the OOP capacity of a solid infill (specimen WE2). Akhoundi et al. (2016) also found that a central window of 80 cm×63.5 cm (12 .8 % area of infill) did not reduce the OOP capacity at all, but the deformation capacity of the infill was reduced significantly, infill collapsed within a small OOP drift (Fig 17). Despite the presence of an opening, the crack pattern indicates that the two-way arching was effective (Fig 18).

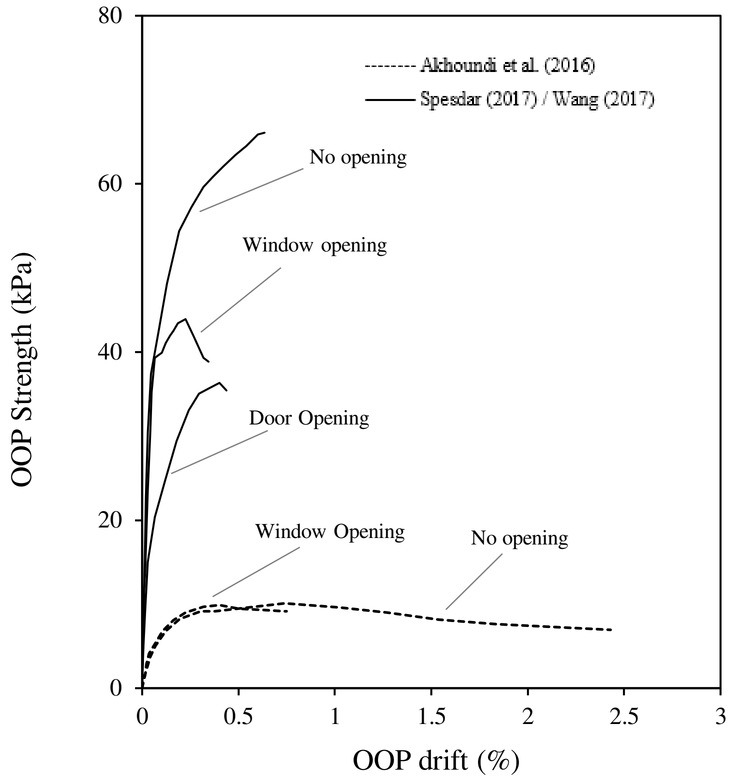

Fig 17. Influence of openings on the OOP capacity of the infill wall

However, experimental studies by Spesdar (2017) and Wang (2017) showed different results. An infill with a centric window (17% area of infill) showed a 35% decrease of capacity while the same infill with a centric door opening measuring 59.2 cm×39.2 cm (17.5% area of infill) in Wang (2017) showed a 45% reduction of the OOP capacity. This is a big reduction in the capacity and it can significantly increase OOP vulnerability of infill walls in earthquakes. The higher reduction of strength in the case of door opening can be associated to a different cracking pattern compared to the case of window opening. Typical diagonal cracking was not observed, which indicates that the two-way arching mechanism was ineffective in the infill wall in the case of door opening (Fig 18).

In the cases of Dawe and Seah (1989), Spesdar (2017) and Wang (2017), the OOP pressure was monotonically increased while in the case of Akhoundi et al. (2016), unidirectional cyclic increasing pressures were applied using an airbag. Since there are not enough tests, it is difficult to connect loading types and the observed OOP behaviour of masonry infill walls.

For infill walls with eccentric opening, the crack patterns due to OOP load (airbag or point loads) on infill walls can be different. However, such tests on infill walls with eccentric opening are not available. Comparison of the cracking patterns in masonry walls having eccentric opening and observed during OOP tests on URM walls (without frames) can be found in Anić et al. (2019).

Moreover, Anić et al. (2021) performed OOP tests on URM infilled frames by applying unidirectional cyclic loads to the top of the infilled frame. Infill specimens with or without opening (centrically and eccentrically positioned window and door) were tested. Since the infilled frames were subjected to bending, infill walls showed cracks parallel to the bed joints. But the cracks were severe in the case of infill with openings, and in the case of eccentric openings, cracks were uneven (Fig 18). These results further indicate that the position of the opening affects the OOP behaviour of infill walls.

Considering that openings are important and a non-avoidable parts of infill wall constructions, investigation in this area has not received a sufficient priority. More tests are deemed necessary to better understand how openings influence the OOP capacity of infill walls.

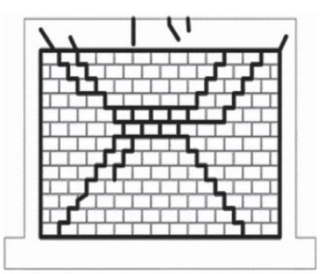

No opening - Akhoundi et al. (2016)

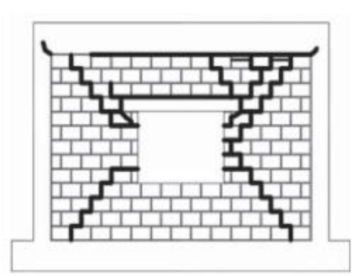

Window opening - Akhoundi et al. (2016)

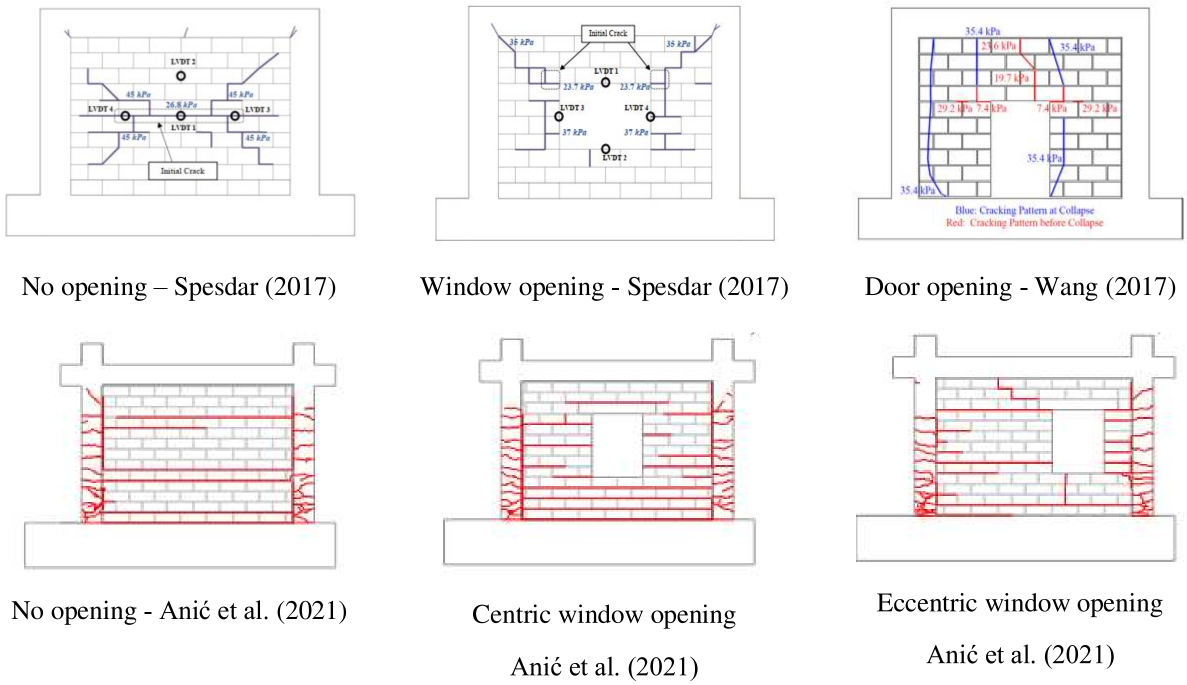

No opening – Spesdar (2017) Window opening - Spesdar (2017) Door opening - Wang (2017)

No opening - Anić et al. (2021) Centric window opening Anić et al. (2021) Eccentric window opening Anić et al. (2021)

Fig 18. Influence of openings in the cracking pattern of infill walls developing due to OOP load

3.6 Effect of vertical load

Very few experimental campaigns have investigated the effect of gravity loads applied over columns on the OOP response of the URM infill, e.g. Angel (1994). In this experimental campaign, an infill specimen without a vertical load (specimen 6t) and a specimen with a vertical load (specimen 6c) of 12.8 kN on each column (producing a stress of 0.14 MPa), were tested in the OOP direction using an airbag pressure. The load-displacement curves of those two specimens were similar to each other; the OOP strength of the masonry infill wall was not much affected. Vertical stress only increased the initial stiffness of the specimen 6c. Angel (1994) also investigated the effect of vertical stress produced in infill due to vertical loads in columns. It was found that with a vertical load of 222.4 kN in each column, the infill carried only 7% of the vertical force on the columns. This was not sufficient to increase the OOP capacity of the infill.

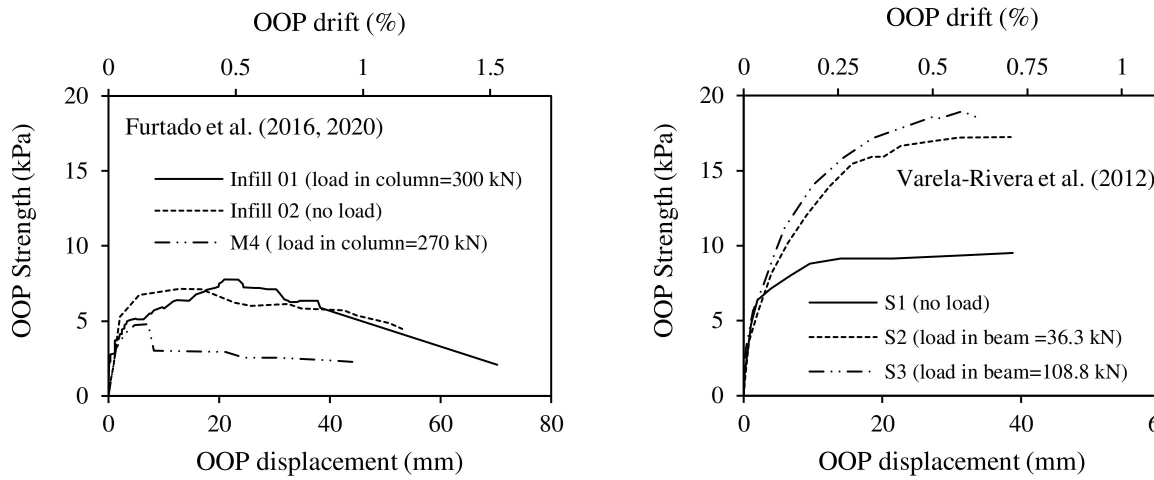

Fig 19. Influence of vertical pre-compression on the OOP capacity of masonry infill walls

Furtado et al. (2016) also tested infill specimens subjected to OOP pressure using an airbag, with and without a vertical load of 300 kN applied over the columns. The specimen with a gravity load i.e. Inf_01 showed slightly higher strength than the one without a gravity load i.e. Inf_02 (Fig 19). Inf_01 was subjected to continuously increasing OOP pressure while Inf_02 was subjected to load-unload cycles of pressure. Infill specimen M4 by Furtado et al. (2020) which was also subjected to unidirectional cyclic loads and a gravity load of 270 kN in the columns showed about 35% lower strength compared to Inf_02. Therefore, the results of the experimental campaigns are contrasting to each other. In one case, Inf_01 with gravity load showed a slightly higher capacity while gravity loaded specimen (M4) exhibited less strength. However, one should not neglect the fact that although infill specimens were built with the same type of materials in Furtado et al. (2016) and Furtado et al. (2020), the mechanical properties were slightly different between the panels. The cracking pattern of M4 showed that interfacial gaps were created between infill and beams at the top and bottom, and vertical cracking was observed almost at mid-span. This indicated that vertical arching was not effective in the infill wall and this could be the primary reason for the decreased strength.

Experimental studies by Varela-Rivera et al. (2012b) showed that a vertical load applied over the top beam influences the OOP capacity of confined masonry walls. The capacity was enhanced when the vertical load was increased (Fig 19). Rabinovitch and Madah (2011) also investigated the OOP behaviour of infill walls under different compression levels applied to the top beam but under dynamic shake table tests. The test results demonstrated that under higher compression the magnitude of the OOP displacement and acceleration were smaller than at lower levels of compression, as a consequence increasing the OOP infill capacity. From what reported above, it is clear univocally the advantageous contribute of vertical stress on infills.

3.7 Effect of surface finish in infill

Experimental studies carried out by Pereira et al. (2011) compared the performance of infill walls made of 150 mm thick masonry units with and without the surface finish. Pereira et al. found that 10 mm plaster without reinforcement on both sides (specimen Wall_REF_02) resulted in about 40 kN (7kPa) OOP lateral strength, while the URM specimen without plaster (Wall_REF_01) showed a peak resistance of only 12 kN (2 kPa). The masonry of infill specimens had similar compressive strength but the one with plaster had higher elastic modulus and shear strength. For the specimen without plaster, the upper frame-infill interface was completely damaged and the upper zone of the wall had a partial or total collapse of the masonry units. Significant OOP tilting of the infill wall at the top level was observed with a horizontal crack at the bottom, indicating cantilever type structural failure. On the other hand, the specimen with the plaster showed a different failure pattern. In particular, there was some damage at the interface between infill and top beam with the formation of horizontal and vertical cracks in the central area of the panel. Diagonal cracking was also observed on the lower half of the panel, indicating the possibility of a two-way arching mechanism. This could be the reason for such a difference in the OOP strength of specimens with and without the application of plaster.

Da Porto et al. (2015) also tested URM infill walls with different types of plaster (ordinary plaster, natural hydraulic lime, lime gypsum plaster) under sequential IP and OOP loads. Additionally, infill specimens with steel meshes in such plasters were tested. In all cases, 120 mm thick masonry units were used and 15 mm thick plaster was applied on both sides of the wall. Types of plasters affected the OOP capacity of the infill walls. In particular, in the case of unreinforced plaster, specimen 1-GP-UR, built with high strength mortar and plastered with low compressive strength ordinary plaster, showed less OOP strength (18.6 kN = 1.7 kPa) compared to specimen 7-BC-UR which was built with low strength mortar and plastered with relatively high strength natural hydraulic lime plaster. The latter showed OOP capacity of 47.4 kN (4.3 kPa). Similarly, specimen 5-BG-UR, which was built with mortar as in specimen 7-BC-UR and plastered with low strength lime gypsum plaster, failed under IP drift (1.2%) and could not be tested in OOP load.

These test results show that the type of plasters can affect the OOP performance of infill walls. It has to be noted that the thickness of plaster (10 mm to 15 mm) used in these tests is also commonly adopted in practice to produce a finished surface in the infill walls. However, there are not enough tests to understand to what degree these surface finishes affect the OOP behaviour of an infill wall. Since plasters are used in almost every wall, it needs further experimental investigations.

3.8 Effect of infill mechanical properties

The OOP strength of infill walls is derived from an arching action, which depends upon the compressive strength of the masonry. The compressive strength of masonry is largely dependent on the strength of the masonry units and mortar. However, only few researchers have investigated the impact on OOP strength due to a change in masonry units, mortar type, or masonry strength in general.

In Angel (1994), specimens 6 and 7 made with clay bricks but with different types of mortar (6 with lime mortar and 7 with type N i.e. cement, lime and sand mixed mortar) showed differences in OOP capacity. Two infill walls had identical geometrical properties (thickness= 98.4 mm). But the strength of the lime mortar was comparatively lower compared to Type N mortar (6.2 MPa in the former and 8.2 MPa in the latter) and the compressive strength of the masonry for specimen 6 was less than half that of specimen 7 and both specimens were subjected to the same amount of prior IP drift (0.25%). Consequently, the OOP strength of specimen 6 was observed to be less than half that of specimen 7.

Moreno-Herera et al. (2016) experimented on infill walls (W1 to W8) built with hollow concrete blocks, hollow clay bricks and solid clay bricks having different compressive strengths but made in equal strength mortar. Experimental results showed OOP strength highly dependent on the compressive strength of masonries. For example, walls W2 and W3 with a different type of unit (compressive strength of 16.3 MPa in the former and 18.9 MPa in the latter) but similar compressive strength of masonry (6.48 MPa in the former and 6.17 MPa in the latter) showed similar OOP strength (10.49 kPa in the former and 11.06 kPa in the latter). However, specimen W1 with masonry units' strength of 6.58 MPa and an average masonry compressive strength of 3.72 MPa had an OOP capacity of only 8.8 kPa.

From the above, it can be understood that with an increase in compressive strength of the mortar, masonry unit and masonry, the OOP capacity of the masonry infill wall increase. But, the available experimental camaigns have focused much less on this aspect. As also highlighted in section 2.1, only in few experimental camapaigns, infill specimens with masonry strength higher than 3 MPa in general for both solid and hollow masonry units, were tested. Therefore, more systematic experimental campaigns in the range of infill masonry properties are necessary to fill the voids in understanding the OOP behaviour of infill walls.

3.9 Effect of surrounding frames

The arching action in infill walls depends on the stiffness of the surrounding frames. This has been understood and thus the effect of frame flexibility has been incorporated in analytical capacity models to define the OOP strength (Dawe and Seah 1989; Angel 1994; Flanagan and Bennett 1999a; Moghadam and Goudarzi 2010). Angel (1994) also defined the criteria of flexural stiffness required for frames to be sufficiently stiff. However, there are not many tests where the effect of frame stiffness is directly investigated. In Spesdar (2017) and Wang (2017), the OOP behaviour of URM infills in RC and steel frames was tested. The OOP capacity in the case of steel frames was significantly lower than in the case of RC frames (Fig 20). According to the authors, the low capacity in the case of steel frames was due to the small bending stiffness of the flange of the steel sections, although the flexural stiffness of the whole steel cross-sections was higher than that of RC cross-sections. The authors also attributed the lower strength to the lower torsional stiffness of the steel frames. The OOP strength of infill walls in steel frames can be influenced by the bonding between the infill and the steel sections, not so effective as in an RC frame. However, this aspect has not been studied experimentally. Further tests with variation in the stiffness of bounding frames can be helpful to understand the stiffness criteria required for the optimum OOP performance of infill walls.

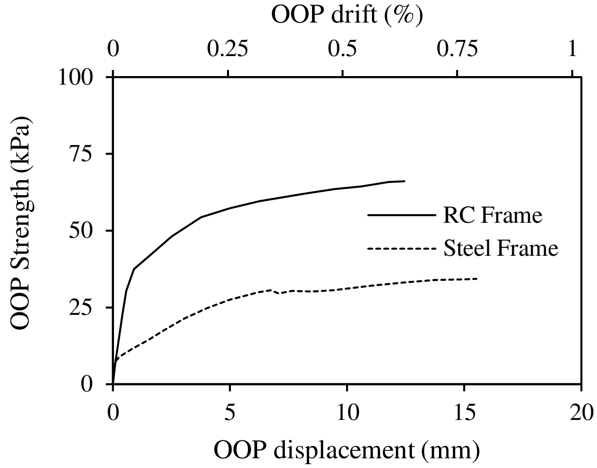

Fig 20. OOP capacity of infills in RC and steel frames by Spesdar (2017) and Wang (2017)

4. OOP damage and its effect on IP capacity

Some experimental campaigns can be found in the literature exploring the infill's IP behaviour after OOP loading. This section is devoted to this subject completing the frame of the OOP tests available in the literature and suggesting a higher influence of IP damage on OOP behaviour with respect to the influence of OOP damage on IP behaviour.

In the research of Flanagan and Bennett (1999b), the level of the influence of OOP damage on IP behaviour is immediately clear. During the experiment, specimen 20 was subjected to increasing OOP pressure (load-unload cycles) using an airbag up to 20.7 kPa and a mid-panel deflection of 10.9 mm. Likewise, specimens 11 and 13 were subjected to OOP lateral drift loads applied to the frame top or to the columns at mid-height. To the specimen 11, a cantilever curvature was applied (restrained base and free top) at a drift of 1.7 % and specimen 13 was first subjected to a beam curvature (restrained base and top) followed by a cantilever curvature at a drift of 1.2%. After application of the OOP load, specimens 11, 13 and 20 were tested under IP cyclic loads until failure. These specimens reached the peak IP strength at lower displacements than the control specimen 2 (Fig 21). Moreover, specimen 13 showed slightly higher initial stiffness than the other specimens and specimen 11 showed less IP capacity comparatively. It is to be noted that specimens 2, 11, 13 and 20 had the same thickness (200 mm). The loss in IP capacity was higher in the case of specimen 11 due to a higher OOP drift applied to the frame. Therefore, OOP drift loads when non-negligible, can modify the IP behaviour of infilled frames.

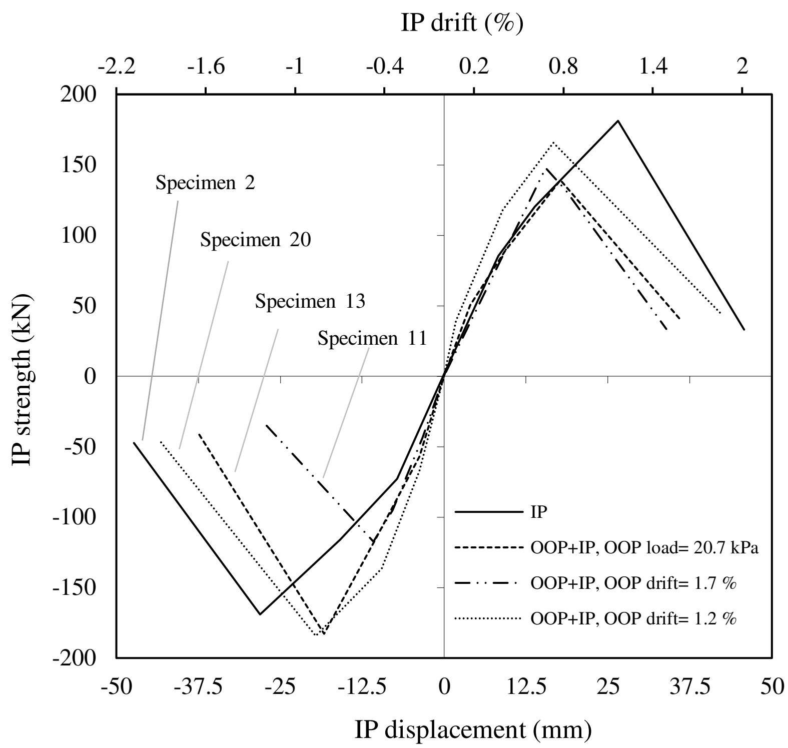

Fig 21. Influence of OOP damage in IP behaviour by Flanagan and Bennett (1999b)

Tests by Henderson et al. (1993) and Spesdar (2017) also showed that the IP capacities were little affected by prior OOP damage. In Henderson et al. (1993), infilled frame was subjected to an OOP cyclic drift load applied to the frame, while in Spesdar (2017), monotonic OOP pressure was applied on the infill, using an airbag. A cyclic IP load was applied in the former case and a monotonic IP load was applied in the latter. The prior OOP damage induced a slight loss of the initial IP stiffness of the specimens in both cases (Fig 22). The reason for the small loss in IP capacity in the case of Henderson et al. (1993) was the small OOP drift (<1%) which caused slight damage in the columns and the infill. Similarly, in the case of Spesdar (2017), OOP load was applied only until the cracking of infill which did not affect the IP performance.

However, Palieraki et al. (2018) showed a decrease of about 20% in IP peak strength due to prior OOP damage. A uniform OOP load was applied in load-unload cycles up to an infill drift of 2.57%, causing a residual OOP displacement. This was the primary reason for the loss of capacity in the IP direction. Further, in the experimental research by Butenweg et al. (2019), a cyclic IP load was applied simultaneously at constant OOP pressure. Although the peak IP strength was slightly higher, the deformation capacity decreased by a factor of around 2 as compared to another specimen affected by IP+OOP+IP loads sequentially applied.

These results indicate that the damage due to loading in the OOP direction of infills can alter the IP capacity of infill walls and the infilled frames. Especially when OOP inter-storey drift loads are applied, the damage in the frames could be higher determining a lower IP capacity (Anić et al. 2021).

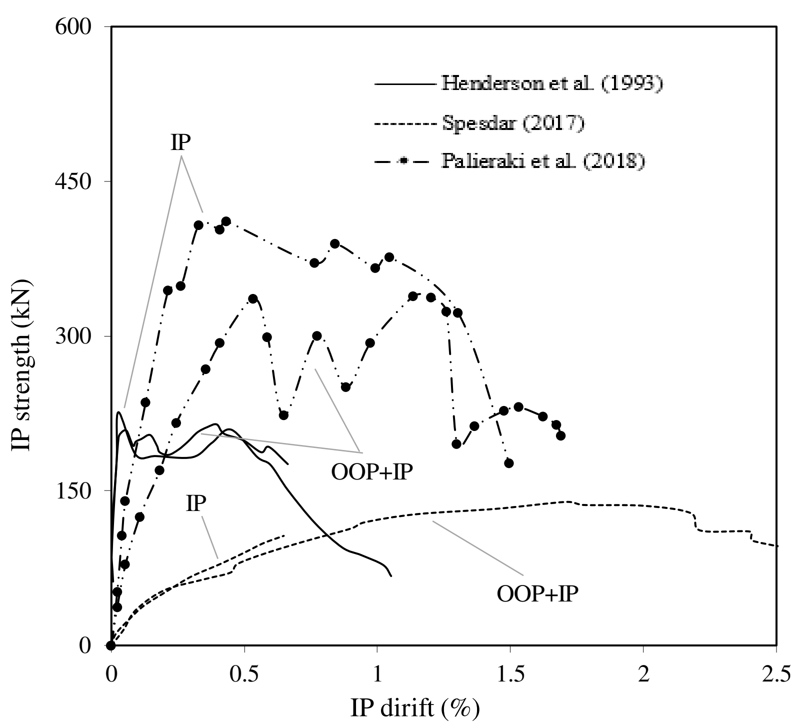

Fig 22. Influence of OOP damage in the IP behaviour of infill walls

5. Conclusion

URM infill walls are important non-structural elements of modern multi-storey frame buildings. The OOP failure of such infills is common during earthquakes and is a big problem even for new buildings designed to resist earthquake forces. Considering the importance of the subject, research on the OOP behaviour of masonry infills is still very limited in comparison to the long research related to their IP behaviour. Nevertheless, the experimental research is increasing in recent years. The analysis of the available tests showed a huge variability in the geometrical and mechanical properties of the infilled frames, making the comparison of the results very difficult. About 80% of the tested infill specimens were built in RC frames and about 60% of them were in full scale. In the majority of the tests (about 85%), infill specimens were built with clay units and in about three-fourth of the tests, specimens were built with hollow masonry units, while in the other one-fourth, solid masonry units were used. The distribution of masonry strength is highly scattered in the case of solid masonry while in the case of hollow masonry, the most of experimental camapigns have used low strength masonry (0 to 4 MPa).

Three-fourth of the experimental camapigns were conducted by using a quasi-static approach while the other one-fourth were performed in dynamic settings using a shake table. In the case of quasi-static method, more than 85% of the tests were conducted by loading the infill walls directly (using airbag or point loads), and in such cases, damage primarily occurs in infill walls. In few tests, OOP inter-storey drift load was used, and in such cases, the damage was concentrated in the frames. Dynamic tests have shown that both infill walls and frames can suffer damage with increasing accelerations. But the number of dynamic tests is very low to make any conclusion.

More experimental tests using inter-storey drift loads and dynamic loads can be very helpful to understand the IP/OOP behaviour of infill walls under earthquake loads.

Studies have revealed that the OOP capacity of masonry infills is primarily influenced by arching effect. The extent of arching depends on the strength of both infill and frame. OOP experimental tests were conducted to understand how different parameters influence arching and consequently infills' OOP behaviour. Experimental campaigns have focused on parameters like slenderness ratio, aspect ratio, boundary conditions, gravity load, masonry strength, openings, surface finish, frame stiffness, etc. From the review of each experiment, it was found that some aspects have received good attention while others need to be deepened.

In general, it seems that all the aspects before mentioned need to be further investigated to properly understand the OOP behaviour of infill walls. But, priority should be given to two major parameters: strength of masonry and infill slenderness ratio. After a proper understanding of the effects of these two parameters, it becomes simpler to know the influence of the other ones. Therefore, tests, possibly in full scale, involving pure OOP load or combined IP and OOP loads, should be increased on URM infill walls having various thicknesses, involving appropriate ranges for the mechanical properties of masonry.

Acknowledgements

The research has been carried out using the resources of ReLUIS (The Laboratories University Network of seismic engineering, Italy) and the support is gratefully acknowledged.

References

Agnihotri, P., Singhal, V., & Rai, D. C. (2013). Effect of in-plane damage on out-of-plane strength of unreinforced masonry walls. Engineering Structures, 57, 1–11.

Akhoundi, F., Vasconcelos, G., Lourenco, P., & Silva, L. (2016). Out-of-plane response of masonry infilled RC frames: Effect of workmanship and opening. In C. Modena, F. da Porto, & M. R. Valluzzi (Eds.), *Brick and Block Masonry* (0 ed., pp. 1147–1154). CRC Press. https://doi.org/10.1201/b21889-143.

Akhoundi, Farhad, Vasconcelos, G., & Lourenço, P. (2020). Experimental Out-Of-Plane Behavior of Brick Masonry Infilled Frames. *International Journal of Architectural Heritage*, *14*(2), 221–237. https://doi.org/10.1080/15583058.2018.1529207.

Angel, R. (1994). *Behavior of reinforced concrete frames with masonry infill walls* (doctoral dissertation). University of Illinois at Urbana-Champaign.

Anić, F., Penava, D., Abrahamczyk, L., & Sarhosis, V. (2020). A review of experimental and analytical studies on the out-of-plane behaviour of masonry infilled frames. *Bulletin of Earthquake Engineering*, *18*(5), 2191–2246. https://doi.org/10.1007/s10518-019-00771-5.

Anić, F., Penava, D., Guljaš, I., Sarhosis, V., & Abrahamczyk, L. (2021). "Out-of-plane cyclic response of masonry infilled RC frames: An experimental study." *Engineering Structures*, 238, 112258.

ASCE (American Society of Civil Engineers). (2017). *Seismic Evaluation and Retrofit of Existing Buildings*. ASCE/SEI 41-17, Reston, VA: ASCE.

Barbosa, A. R., Fahnestock, L. A., Fick, D. R., Gautam, D., Soti, R., Wood, R., Moaveni, B., Stavridis, A., Olsen, M. J., & Rodrigues, H. (2017). Performance of Medium-to-High Rise Reinforced Concrete Frame Buildings with Masonry Infill in the 2015 Gorkha, Nepal, Earthquake. *Earthquake Spectra, 33(1_suppl)*, 197–218. https://doi.org/10.1193/051017eqs087m.

Bashandy, T., Rubiano, N. R., & Klingner, R. E. (1995). *Evaluation and Analytical Verification of Infilled frame Test data* (PMFSEL Report NO.95-1). University of Texas at Austin.

Butenweg, C., Marinković, M., & Salatić, R. (2019). Experimental results of reinforced concrete frames with masonry infills under combined quasi-static in-plane and out-of-plane seismic loading. *Bulletin of Earthquake Engineering*, *17*(6), 3397–3422. https://doi.org/10.1007/s10518-019-00602-7.

Calvi, G. M., & Bolognini, D. (2001). Seismic response of reinforced concrete frames infilled with weakly reinforced masonry panels. *Journal of Earthquake Engineering*, *5*(2), 153–185. https://doi.org/10.1080/13632460109350390.

Cavaleri, L., Fossetti, M., & Papia, M. (2005). Infilled frames: Developments in the evaluation of cyclic behaviour under lateral loads. *Structural Engineering and Mechanics*, 21(4), 469–494.

Cavaleri, L., Fossetti, M., & Papia, M. (2009). Modeling of out-of-plane behavior of masonry walls. Journal of Structural Engineering, ASCE. 135(12), 1522–1532.

Cavaleri, L., Zizzo, M., & Asteris, P. G. (2019). Residual out-of-plane capacity of infills damaged by in-plane cyclic loads. Engineering Structures, 109957.

Corte, D.G., Fiorino, L., & Mazzolani, F. (2008). Lateral-loading tests on a real RC building including masonry infill panels with and without FRP strengthening. *Journal of Materials in Civil Engineering*, 20, 419–431.

da Porto, .F, Guidi, G., Benetta, M.D., & Verlato, N. (2013). Combined In-Plane/Out-of-Plane Experimental Behaviour of Reinforced and Strengthened Infill Masonry Walls. *The Masonry Society, ed. 12th Canadian Masonry Symposium*.

da Porto, F., Donà, M., Verlato, N., & Guidi, G. (2020). "Experimental Testing and Numerical Modeling of Robust Unreinforced and Reinforced Clay Masonry Infill Walls, With and Without Openings." *Frontiers in Built Environment*, 6, 591985.

da Porto, F., Guidi, G., Verlato, N., & Modena, C. (2015). Effectiveness of plasters and textile reinforced mortars for strengthening clay masonry infill walls subjected to combined in-plane/out-of-plane actions / Wirksamkeit von Putz und textilbewehrtem Mörtel bei der Verstärkung von Ausfachungswänden aus Ziegel: Effectiveness of plasters and textile reinforced mortars for strengthening clay masonry infill walls subjected to combined in-plane/out-of-plane actio. *Mauerwerk*, *19*(5), 334–354. https://doi.org/10.1002/dama.201500673.

Dawe, J. L., & Seah, C. K. (1989). Out-of-plane resistance of concrete masonry infilled panels. *Canadian Journal of Civil Engineering*, *16*(6), 854–864. https://doi.org/10.1139/l89-128.

De Risi, M. T., Di Domenico, M., Ricci, P., Verderame, G. M., & Manfredi, G. (2019). Experimental investigation on the influence of the aspect ratio on the in-plane/out-of-plane interaction for masonry infills in RC frames. *Engineering Structures*, *189*, 523–540. https://doi.org/10.1016/j.engstruct.2019.03.111.

Di Domenico, M., De Risi, M. T., Ricci, P., Verderame, G. M., & Manfredi, G. (2021). Empirical prediction of the in-plane/out-of-plane interaction effects in clay brick unreinforced masonry infill walls. *Engineering Structures*, 227, 111438.

Di Domenico, M., Ricci, P., & Verderame, G. M. (2018). Experimental Assessment of the Influence of Boundary Conditions on the Out-of-Plane Response of Unreinforced Masonry Infill Walls. *Journal of Earthquake Engineering*, *24*(6), 881–919. https://doi.org/10.1080/13632469.2018.1453411.

Di Domenico, M., Ricci, P., & Verderame, G. M. (2019a). Experimental assessment of the out-of-plane strength of URM infill walls with different slenderness and boundary conditions. *Bulletin of Earthquake Engineering*, *17*(7), 3959–3993. https://doi.org/10.1007/s10518-019-00604-5.

Di Domenico, M., Ricci, P., & Verderame, G. M. (2019b). Predicting the Out-Of-Plane Seismic Strength of Unreinforced Masonry Infill Walls. *Journal of Earthquake Engineering*, 1–38. https://doi.org/10.1080/13632469.2019.1604453.

Eurocode 6 (2005). *Design of Structures for Earthquake Resistance, Part 1: General rules, seismic actions and rules for buildings Masonry Structures,* European Committee for Standardization; Brussels, Belgium.

Eurocode 8 (2004). *Design of structures for Earthquake Resistance, Part 1-1: General Rules, Seismic Actions and Rules for Buildings*, European Committee for Standardization, Brussels.

Fardis, M. N., Bousias, S. N., Franchioni, G., & Panagiotakos, T. B. (1999). *Seismic response and design of RC structures with plan-eccentric masonry infills*. 19.

Flanagan, R. D., & Bennett, R. M. (1999a). Arching of Masonry Infilled Frames: Comparison of Analytical Methods. *Practice Periodical on Structural Design and Construction*, *4*(3), 105–110. https://doi.org/10.1061/(ASCE)1084-0680(1999)4:3(105).

Flanagan, R. D., & Bennett, R. M. (1999b). Bidirectional Behavior of Structural Clay Tile Infilled Frames. *Journal of Structural Engineering*, *125*(3), 236–244. https://doi.org/10.1061/(ASCE)0733-9445(1999)125:3(236).

Fowler, J.J. (1994). *Analysis of dynamic testing performed on structural clay tile infilled frames* (Doctoral dissertation) Oak Ridge National Lab.(ORNL), Oak Ridge, TN (United States).

Frederiksen, V. (1992). Membrane effect in laterally loaded masonary walls. A second order phenomenon. *in Proceedings of the 6th Canadian Masonry Symposium.* University of Saskatchewan, Saskatoon, Canada.

Furtado, A., Rodrigues, H., Arêde, A., & Varum, H. (2016). Experimental evaluation of out-of-plane capacity of masonry infill walls. *Engineering Structures*, *111*, 48–63. https://doi.org/10.1016/j.engstruct.2015.12.013.

Furtado, A., Rodrigues, H., Arêde, A., & Varum, H. (2018). Out-of-plane behavior of masonry infilled RC frames based on the experimental tests available: A systematic review. *Construction and Building Materials*, *168*, 831–848. https://doi.org/10.1016/j.conbuildmat.2018.02.129.

Furtado, A., Rodrigues, H., Arêde, A., & Varum, H. (2020). Effect of the Panel Width Support and Columns Axial Load on the Infill Masonry Walls Out-Of-Plane Behavior. *Journal of Earthquake Engineering*, *24*(4), 653–681. https://doi.org/10.1080/13632469.2018.1453400.

Gesualdi, G., Viggiani, L. R. S., & Cardone, D. (2020). "Seismic performance of RC frame buildings accounting for the out-of-plane behavior of masonry infills." *Bulletin of Earthquake Engineering*, 18(11), 5343–5381.

Hak, S., Morandi, P., & Magenes, G. (2014.). *Out-of-plane experimental response of strong masonry infills*. In: 2nd European conference on earthquake engineering and seismology, 12.

Henderson, R., Jones, W., Burdette, E., & Porter, M. (1993). The effect of prior out-of-plane damage on the in-plane behavior of unreinforced masonry infilled frames. *In: The Fourth DOE Natural Phenomena Hazards Mitigation Conference*.

Hermanns, L., Fraile, A., Alarcón, E., & Álvarez, R. (2014). Performance of buildings with masonry infill walls during the 2011 Lorca earthquake. *Bulletin of Earthquake Engineering, 12(5)*, 1977–1997. https://doi.org/10.1007/s10518-013-9499-3.

Ingham, J., Walsh, K., Dizhur, D., & Shafaei, J. (2014). *Out-of-plane testing of unreinforced brick infill walls within structural frames*. (Final Report – LR0441) https://doi.org/10.13140/RG.2.1.4750.0245.

Kadysiewski, S., & Mosalam, K. M. (2009). Modeling of Unreinforced Masonry Infill Walls Considering In-Plane and Out-of-Plane Interaction. PEER 2008/102, University of California, Berkeley, 144.

Klingner, R.E., Rubiano N.R., Bashandy, T.R., & Sweeney, S.C. (1996). Evaluation and analytical verification of shaking table data from infilled frames, part 2: Out-of-plane behavior. *In: Proceedings of the 7th North American Masonry Conference* (pp. 521-532), Colorado: Elsevier Science Ltd.

Komaraneni, S., Rai, D. C., & Singhal, V. (2011). Seismic Behavior of Framed Masonry Panels with Prior Damage When Subjected to Out-of-Plane Loading. *Earthquake Spectra*, *27*(4), 1077–1103. https://doi.org/10.1193/1.3651624.

Koutas, L. N., & Bournas, D. A. (2019). Out-of-Plane Strengthening of Masonry-Infilled RC Frames with Textile-Reinforced Mortar Jackets. *Journal of Composites for Construction*, *23*(1), 04018079. https://doi.org/10.1061/(ASCE)CC.1943-5614.0000911.

Liauw, T. C., & Kwan, A. K. H. (1992). Experimental study of shear wall and infilled frame on shake table. *Earthquake Engineering,Tenth World Conference*.

Liberatore, L., AlShawa, O., Marson, C., Pasca, M., & Sorrentino, L. (2020). Out-of-plane capacity equations for masonry infill walls accounting for openings and boundary conditions. Engineering Structures, 207, 110198.

Liu, M., Cheng, Y., & Liu, X. (2011). Shaking table test on out-of-plane stability of infill masonry wall. *Transactions of Tianjin University*, *17*(2), 125–131. https://doi.org/10.1007/s12209-011-1534-3

Lunn, D. S., & Rizkalla, S. H. (2011). Strengthening of Infill Masonry Walls with FRP Materials. *Journal of Composites for Construction*, *15*(2), 206–214. https://doi.org/10.1061/(ASCE)CC.1943-5614.0000088.

McDowell, .EL., McKee, K.E. & Sevin. E. (1956). Discussion of arching action theory of masonry walls. *Proceedings of American Society of Civil Engineering Journal Structural Division* 82 (pp. 27–40).

Mehrabi, A.B., Shing, P.B., Schuller, M.P., & Noland, J.L. (1996) Experimental evaluation of masonry-infilled RC frames. *Journal of Structural Engineering*, ASCE, 122(3), pp. 228–237.

Milanesi, R. R., Morandi, P., Manzini, C. F., Albanesi, L., & Magenes, G. (2020). Out-of-plane Response of an Innovative Masonry Infill with Sliding Joints from Shaking Table Tests. *Journal of Earthquake Engineering*, 1–35. https://doi.org/10.1080/13632469.2020.1739173.

Misir, I. S., Ozcelik, O., Girgin, S. C., & Yucel, U. (2016). The Behavior of Infill Walls in RC Frames Under Combined Bidirectional Loading. *Journal of Earthquake Engineering*, *20*(4), 559–586. https://doi.org/10.1080/13632469.2015.1104748.

Moghadam, H., & Goudarzi, N. (2010). Transverse Resistance of Masonry Infills. *ACI Structural Journal*, 7.

Moghaddam H., Dowling P., & Ambraseys N. (1988). Shaking table study of brick masonry infilled frames subjected to seismic actions. *in 9th World Conference on Earthquake Engineering*. Tokyo.

Moreno-Herrera, J., Varela-Rivera, J., & Fernandez-Baqueiro, L. (2016). Out-of-Plane Design Procedure for Confined Masonry Walls. *Journal of Structural Engineering*, *142*(2), 04015126. https://doi.org/10.1061/(ASCE)ST.1943-541X.0001391.

Moșoarcă, M., Petrus, C., Stoian, V., & Anastasiadis, A. (2016). Behaviour of masonry infills subjected to out of plane seismic actions. Part 2: Experimental testing. In: Modena C, da Porto F, Valluzzi MR (Eds)*, Brick Block Mason. 0 ed., CRC Press*, (pp. 1293–300).

Onat, O., Correia, A. A., Lourenço, P. B., & Koçak, A. (2018). Assessment of the combined in-plane and out-of-plane behavior of brick infill walls within reinforced concrete frames under seismic loading. *Earthquake Engineering & Structural Dynamics*, *47*(14), 2821–2839. https://doi.org/10.1002/eqe.3111.

Palieraki, V., Zeris, C., Vintzileou, E., & Adami, C.-E. (2018). In-plane and out-of plane response of currently constructed masonry infills. *Engineering Structures*, *177*, 103–116. https://doi.org/10.1016/j.engstruct.2018.09.047.

Pantò, B., Silva, L., Vasconcelos, G., & Lourenço, P. B. (2019). Macro-modelling approach for assessment of out-of-plane behavior of brick masonry infill walls. *Engineering Structures*, *181*, 529–549. https://doi.org/10.1016/j.engstruct.2018.12.019.

Pasca M., Liberatore L. & Masiani R. (2017). Reliability of analytical models for the prediction of out-of-plane capacity of masonry infills. *Structural Engineering and Mechanics*, 64(6), 765–781.

Pereira, M.F.P., Pereira, M.F.N., Ferreira, J.E.D., & Lourenço, P.B. (2011). Behaviour of masonry infill panels in RC frames subjected to in plane and out of plane loads. *in: 7th International Conference on Analytical Models and New Concepts in Concrete and Masonry Structures*.

Petrus, C., Stoian, V., Moșoarcă, M., & Anastasiadis, A. (2011). Reinforced Concrete Frames with Masonry Infills. Out of Plane Experimental Investigation. *Civil Engineering*, 11.

Pradhan, B., Sarhosis, V., Ferrotto, M.F., Penava, D. & Cavaleri, L. (2021). Prediction Equations for the Out-of-Plane Capacity of Unreinforced Masonry Infill Walls Based on a Macro-element

Model Parametric Analysis. *Journal of Engineering Mechanics ASCE*. 10.1061/(ASCE)EM.1943-7889.0001998.

Preti, M., Migliorati, L., & Giuriani, E. (2015). Experimental testing of engineered masonry infill walls for post-earthquake structural damage control. *Bulletin of Earthquake Engineering*, *13*(7), 2029–2049. https://doi.org/10.1007/s10518-014-9701-2.

Rabinovitch, O., & Madah, H. (2011). Finite element modeling and shake-table testing of unidirectional infill masonry walls under out-of-plane dynamic loads. *Engineering Structures*, *33*(9), 2683–2696. https://doi.org/10.1016/j.engstruct.2011.05.019.

Ricci P., Di Domenico M., & Verderame G.M. (2018c). Empirical-based out-of-plane URM infill wall model accounting for the interaction with in-plane demand." Earthquake Eng Struct Dyn. 2018a; 4, 802–827.

Ricci, P., De Luca, F., & Verderame, G. M. (2011). 6th April 2009 L'Aquila earthquake, Italy: Reinforced concrete building performance. *Bulletin of Earthquake Engineering, 9(1),* 285–305. https://doi.org/10.1007/s10518-010-9204-8.

Ricci, P., Di Domenico, M., & Verderame, G. M. (2018a). Experimental assessment of the in-plane/out-of-plane interaction in unreinforced masonry infill walls. *Engineering Structures*, *173*, 960–978. https://doi.org/10.1016/j.engstruct.2018.07.033.

Ricci, P., Di Domenico, M., & Verderame, G. M. (2018b). Experimental investigation of the influence of slenderness ratio and of the in-plane/out-of-plane interaction on the out-of-plane strength of URM infill walls. *Construction and Building Materials*, *191*, 507–522. https://doi.org/10.1016/j.conbuildmat.2018.10.011.

Ricci, P., Di Domenico, M., & Verderame, G. M. (2020). "Effects of the In-Plane/Out-of-Plane Interaction in URM Infills on the Seismic Performance of RC Buildings Designed to Eurocodes." *Journal of Earthquake Engineering*, 1–35.

Sagar, S. L., Singhal, V., & Rai, D. C. (2019). In-Plane and Out-of-Plane Behavior of Masonry-Infilled RC Frames Strengthened with Fabric-Reinforced Cementitious Matrix. *Journal of Composites for Construction*, *23*(1), 04018073. https://doi.org/10.1061/(ASCE)CC.1943-5614.0000905.

Silva, L., Vasconcelos, G., Lourenço, P., & Akhoundi, F. (2016). Experimental evaluation of a constructive system for earthquake resisting masonry enclosure walls. In C. Modena, F. da Porto, & M. R. Valluzzi (Eds.), *Brick and Block Masonry* (0 ed., pp. 1333–1340). CRC Press. https://doi.org/10.1201/b21889-165.

Singhal, V., & Rai, D. C. (2016). In-plane and out-of-plane behavior of confined masonry walls for various toothing and openings details and prediction of their strength and stiffness: Behavior of Confined Masonry Walls and Predictions of Their Response. *Earthquake Engineering & Structural Dynamics*, *45*(15), 2551–2569. https://doi.org/10.1002/eqe.2783.

Spesdar, R. (2017). Experimental investigation on the out-of-plane behaviour of the concrete masonry infilled RC frames [Master's thesis]. Dalhousie University https://dalspace.library.dal.ca/handle/10222/72875.

Tondelli, M., Beyer, K., & DeJong, M. (2016). Influence of boundary conditions on the out-of-plane response of brick masonry walls in buildings with RC slabs: Out-of-plane Response of Masonry Walls in Buildings with RC Slabs. *Earthquake Engineering & Structural Dynamics*, *45*(8), 1337–1356. https://doi.org/10.1002/eqe.2710.

Tu, Y.-H., Chuang, T.-H., Liu, P.-M., & Yang, Y.-S. (2010). Out-of-plane shaking table tests on unreinforced masonry panels in RC frames. *Engineering Structures*, 32(12), 3925–3935. https://doi.org/10.1016/j.engstruct.2010.08.030.

Tu, Y.-H., Liu, P.-M., & Lin, H.-P. (2007). Out-of-Plane Seismic Behavior of Unreinforced Masonry In-filled Walls. *New Horizons and Better Practices*, 1–10. https://doi.org/10.1061/40946(248)48.

Vailati, M., Monti, G., & Di Gangi, G. (2018). Earthquake-Safe and Energy-Efficient Infill Panels for Modern Buildings. In R. Rupakhety & S. Ólafsson (Eds.), *Earthquake Engineering and Structural Dynamics in Memory of Ragnar Sigbjörnsson* (Vol. 44, pp. 233–261). Springer International Publishing. https://doi.org/10.1007/978-3-319-62099-2_12.

Varela-Rivera, J. L., Navarrete-Macias, D., Fernandez-Baqueiro, L. E., & Moreno, E. I. (2011). Out-of-plane behaviour of confined masonry walls. *Engineering Structures*, 33(5), 1734–1741. https://doi.org/10.1016/j.engstruct.2011.02.012.

Varela-Rivera, J., Moreno-Herrera, J., Lopez-Gutierrez, I., & Fernandez-Baqueiro, L. (2012a). Out-of-Plane Strength of Confined Masonry Walls. *Journal of Structural Engineering*, 138(11), 1331–1341. https://doi.org/10.1061/(ASCE)ST.1943-541X.0000578.

Varela-Rivera, J., Polanco-May, M., Fernandez-Baqueiro, L., & Moreno, E. I. (2012b). Confined masonry walls subjected to combined axial loads and out-of-plane uniform pressures. *Canadian Journal of Civil Engineering*, 39(4), 439–447. https://doi.org/10.1139/l2012-021.

Varum, H., Furtado, A., Rodrigues, H., Dias-Oliveira, J., Vila-Pouca, N., & Arêde, A. (2017). Seismic performance of the infill masonry walls and ambient vibration tests after the Ghorka 2015, Nepal earthquake. *Bulletin of Earthquake Engineering,* 15(3), 1185–1212. https://doi.org/10.1007/s10518-016-9999-z.

Verlato, N., Guidi, G., da Porto, F., & Modena, C. (2016). Innovative systems for masonry infill walls based on the use of deformable joints: Combined in-plane/out-of-plane tests. In C. Modena, F. da Porto, & M. R. Valluzzi (Eds.), *Brick and Block Masonry* (0 ed., pp. 1359–1366). CRC Press. https://doi.org/10.1201/b21889-168.

Wang, C. (2017). Experimental investigation on the out-of-plane behaviour of concrete masonry infilled frames [Master's thesis]. Dalhousie University https://dalspace.library.dal.ca/handle/10222/73415.

Wang, X., Zhao, W., Kong, J., and Zhao, T. (2020). Numerical Investigation on the Influence of In-Plane Damage on the Out-of-Plane Behavior of Masonry Infill Walls. *Advances in Civil Engineering*, 2020, 1–16.

Wu, J., Zhang, L., Yu, Q., and Wang, B. (2020). Out-of-Plane Shaking Table Tests on Seismic Response of RC Frame Infilled with a New Type of Shale Fired Heat-Insulation Blocks. *Advances in Materials Science and Engineering*, 2020, 1–13.

Zarnic, R., Gostic, S., Crewe, A. J., & Taylor, C. A. (2001). Shaking table tests of 1:4 reduced-scale models of masonry infilled reinforced concrete frame buildings. *Earthquake Engineering & Structural Dynamics*, *30*(6), 819–834. https://doi.org/10.1002/eqe.39.